Non-destructive defect imaging in the SEM

Yoosuf N. Picard
Associate Research Professor
Department of Materials Science and Engineering
Carnegie Mellon University, Pittsburgh, USA

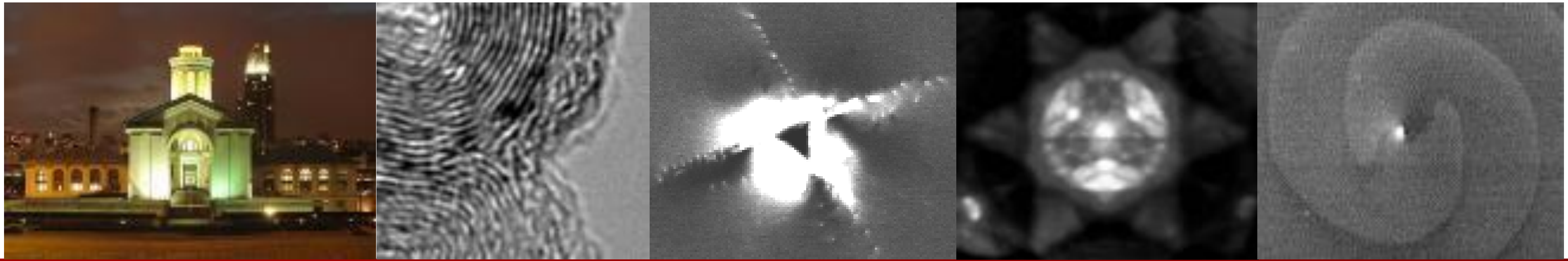

Types of Defects

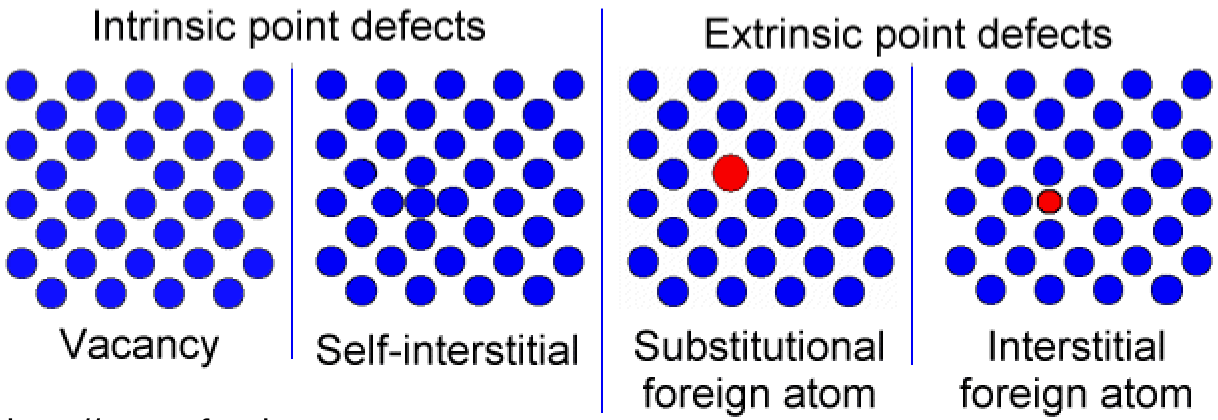

http://www.tf.uni-kiel.de/matwis/amat/iss/kap_5/illustr/gang_of_four_lettered.gif

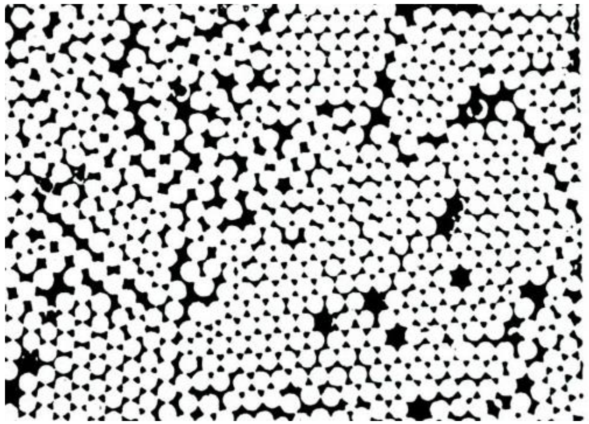

http://cmcintyre.com/blog/crystal-structure

Screw line defect

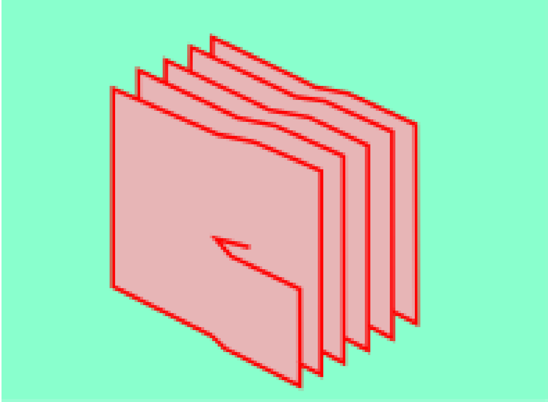

Edge line defect

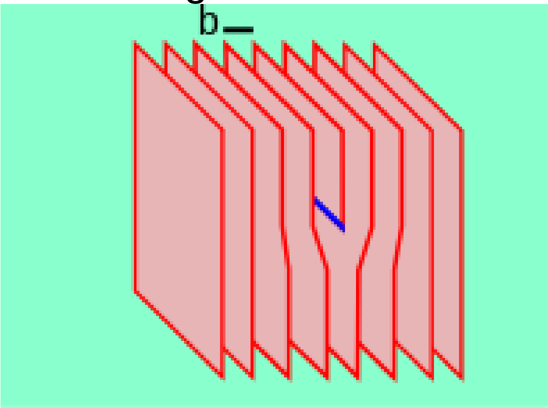

https://en.wikipedia.org/wiki/Dislocation

Volumetric defects

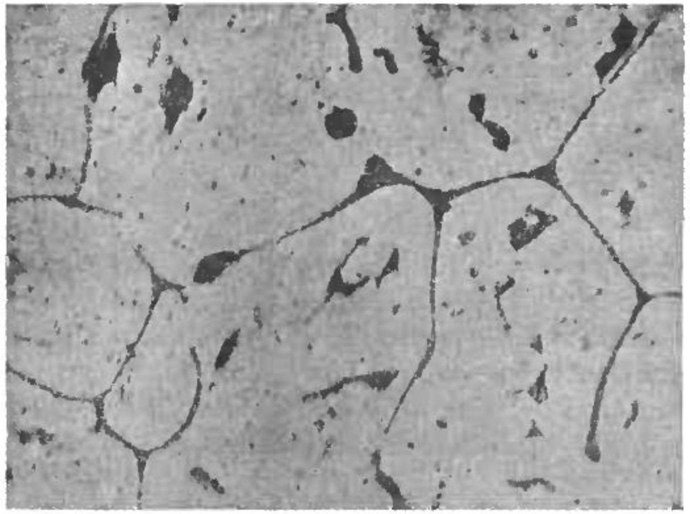

https://commons.wikimedia.org/wiki/File:Metallography_of_iron_FeS_inclusions.PNG

Line defects: Dislocations

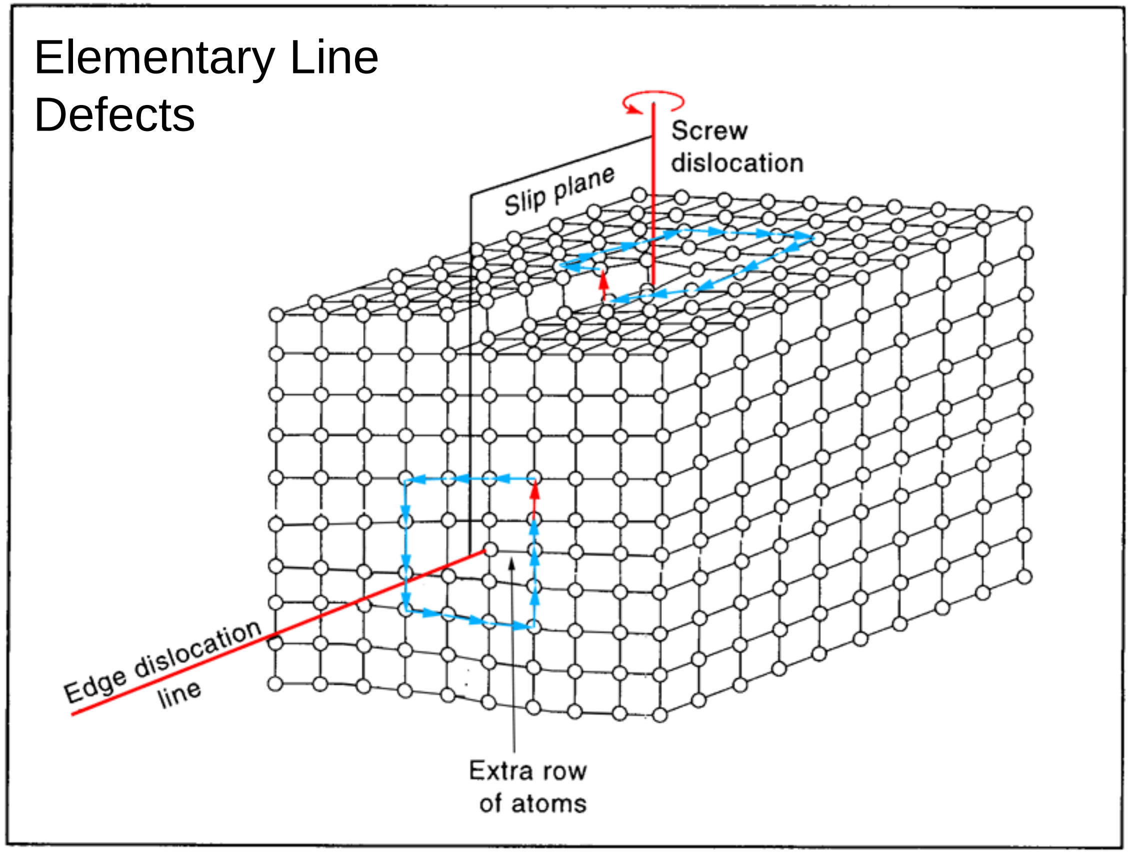

u: dislocation line

b: Burgers vector

Screw: **u** ∥ **b**

Edge: **u** ⊥ **b**

If you determine **b** and **u**, you have identified the dislocation

Dislocation creation, motion, annihilation, and properties (electrical, optical) are function of dislocation type and line direction

Line Defects – Current Issues

Dislocations continue to influence critical aspects related to device performance – solar cells, LEDS

Non-destructive methods for locating and identifying dislocations remain critical

Dislocations as Memristors in $SrTiO_3$

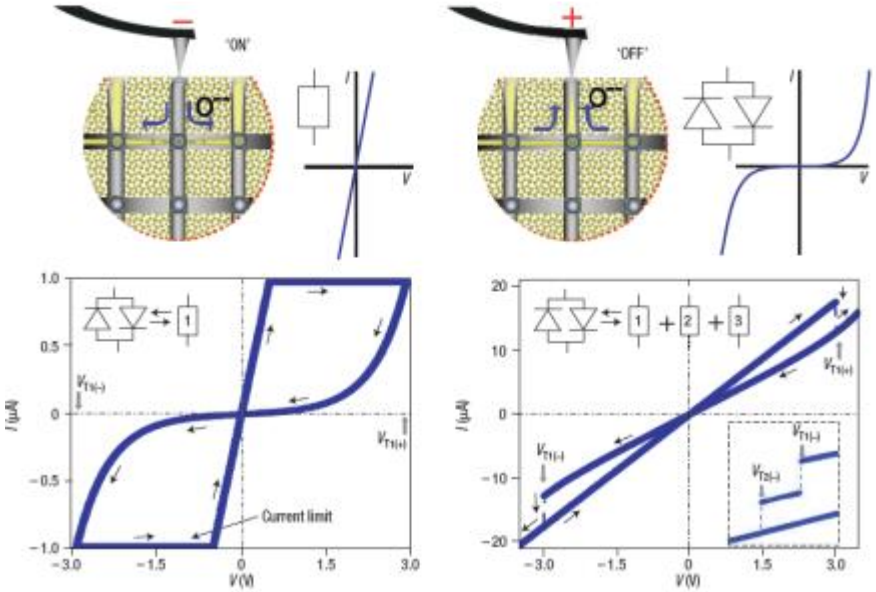

K. Szot *et al*, Nature Materials. **5**, 312 (2006).

Multicrystalline Si solar cells

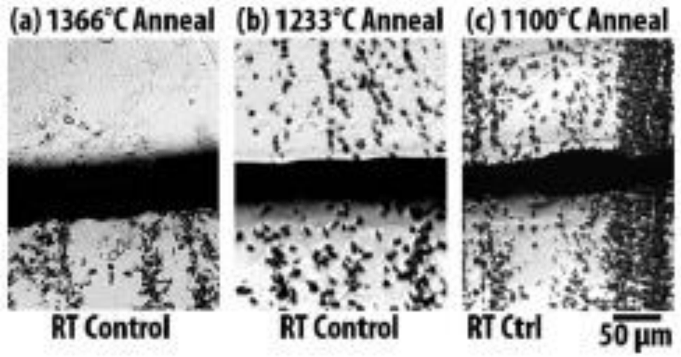

K. Hartman *et al*, Appl. Phys. Lett. **93**, 122108 (2008).

III-V multijunction solar cells

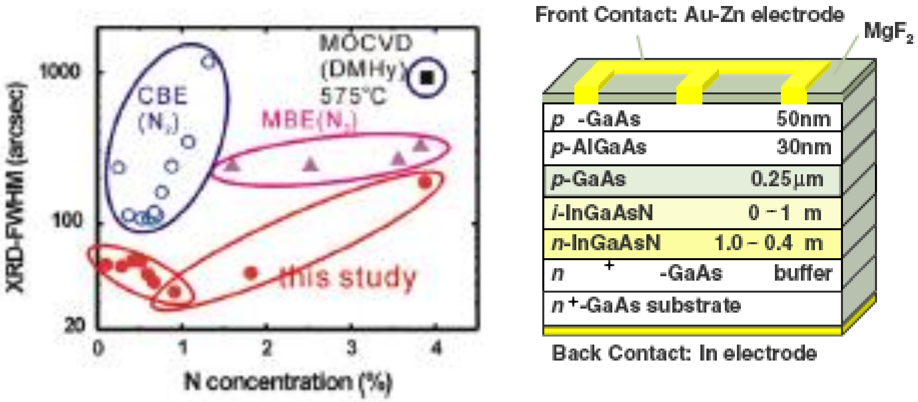

M. Yamaguchi *et al,* Solar Energy **82**, 173 (2008).

Present Dislocation Imaging Approaches

Various techniques suffer certain limitations:

TEM – destructive, confined area

XRD – not local but global

SWBXT - requires a synchrotron x-ray source

AFM - contact, indirectly images dislocations

Chemical etching - destructive

Luminescence (CL, PL, EL) –
little surface information,
may require pre-processing,
requires pre-existing knowledge of optical behavior

<u>Dislocation Density → Average Dislocation Separation</u>

$10^8/cm^2$ → 1 μm $\quad$ $10^5/cm^2$ → 32 μm

X-TEM of AlN

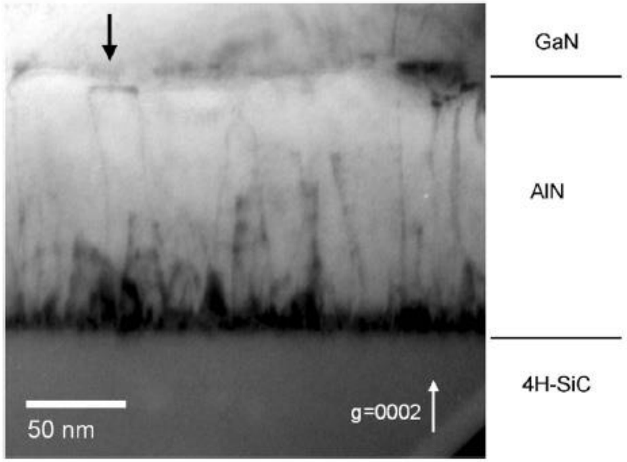

Y.N. Picard *et al*, Appl. Phys. Lett. **91**, 014101 (2007).

AFM of MBE GaN

B. Heying *et al*, J. Appl. Phys. **85**, 6470 (1999).

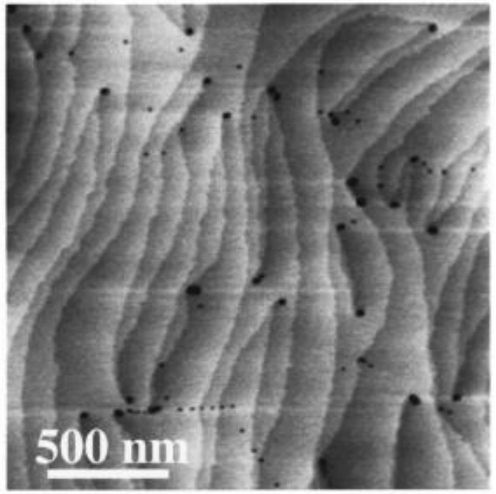

Electron Channeling Contrast Imaging (ECCI)

ECCI image of MOCVD GaN film

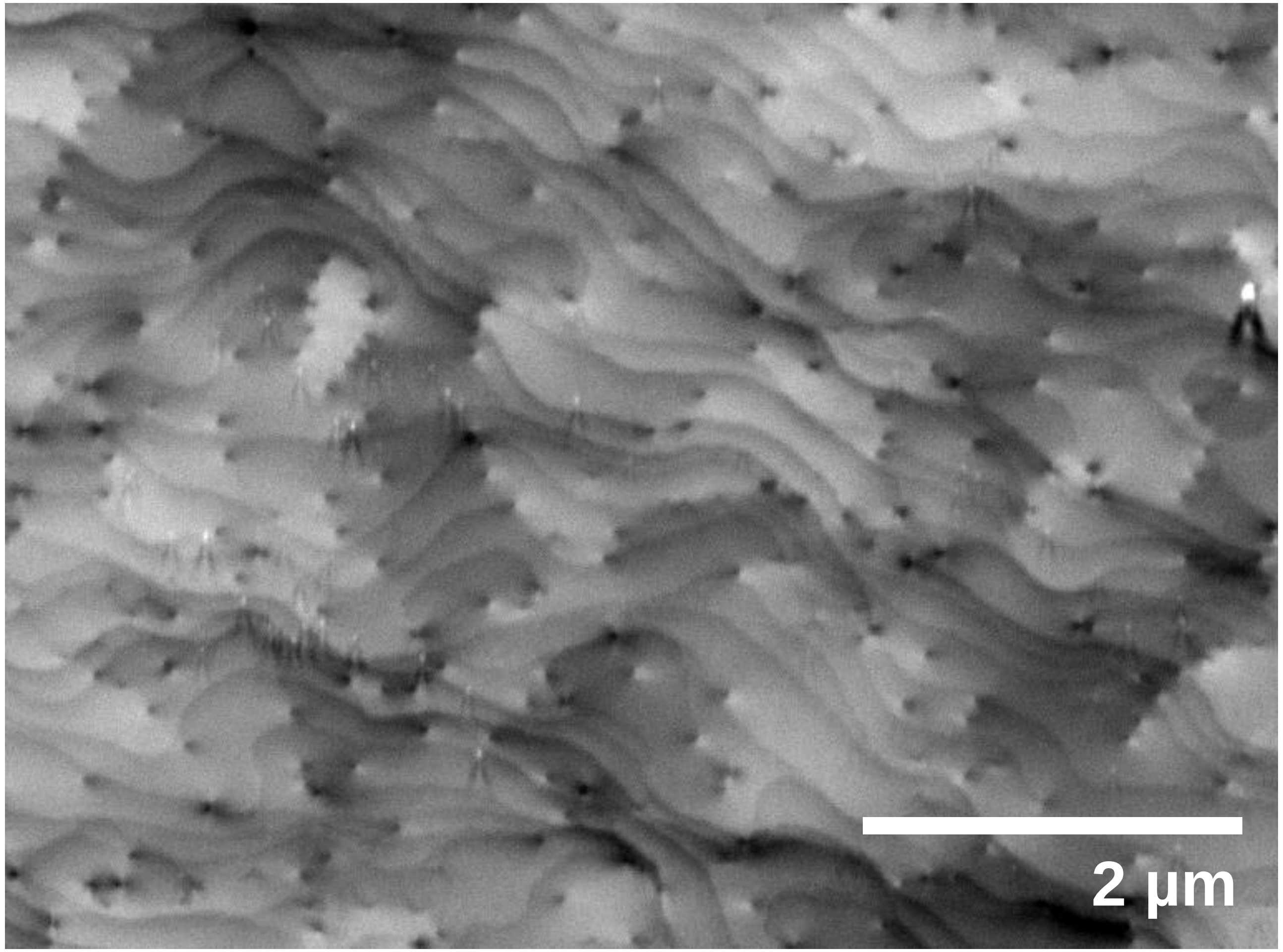

- Non-destructive
- Non-contact
- Commercial SEM
- Dislocation imaging
- Atomic morphology
- Orientation contrast
- Phase identification

Electron Channeling

η: backscattered electron yield

η is a strong function of the relative orientation between incident electron beam and crystal

Discovered by D.G. Coates, Phil. Mag. 16, 1179 (1967).

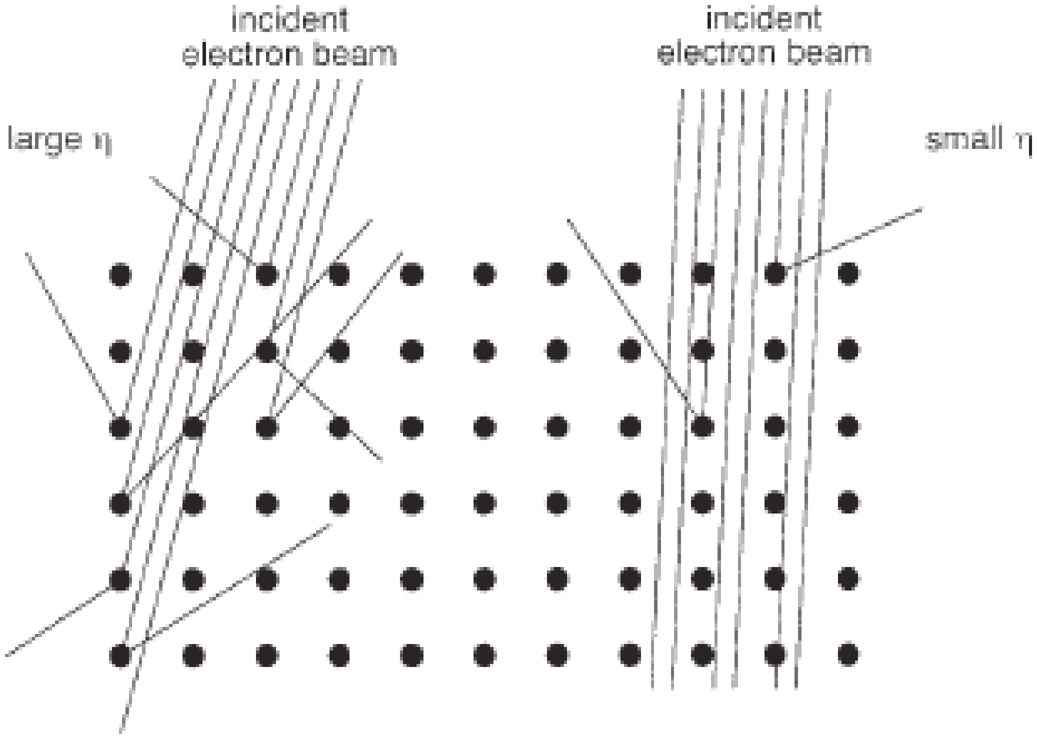

Fig. 1. Schematic representation of the variation in back scattered electron emission (η) as a function of the relative orientation between the incident electron beam and the crystal lattice (after Joy et al. 1982).

David C. Joy, Dale E. Newbury, and David L. Davidson. "Electron channeling patterns in the scanning electron microscope." *Journal of Applied Physics*53.8 (1982): R81-R122.

Diffraction in the SEM

Electron Backscatter Diffraction (EBSD)

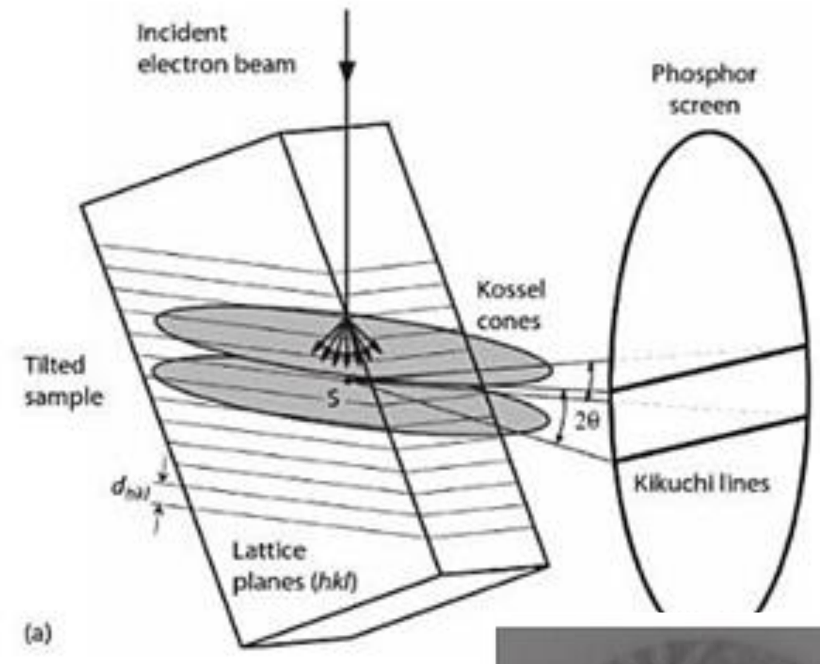

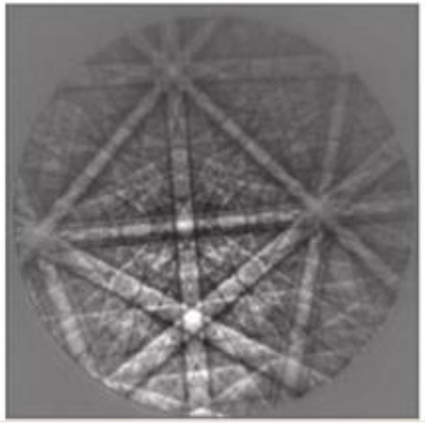

Electron Channeling Pattern (ECP)

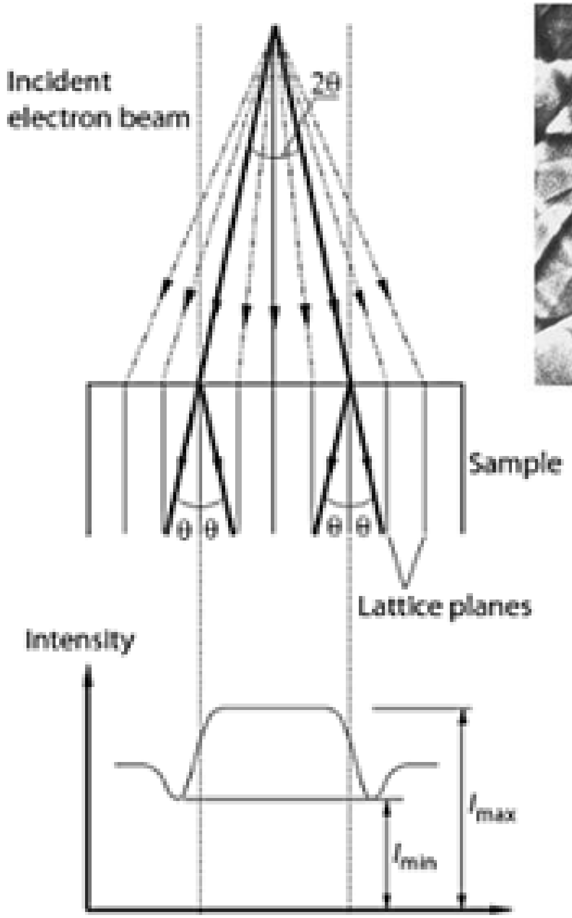

O. Engler and V. Randle, Introduction to Texture Analysis, 2nd. Edition, CRC Press 2009

Channeling in the SEM

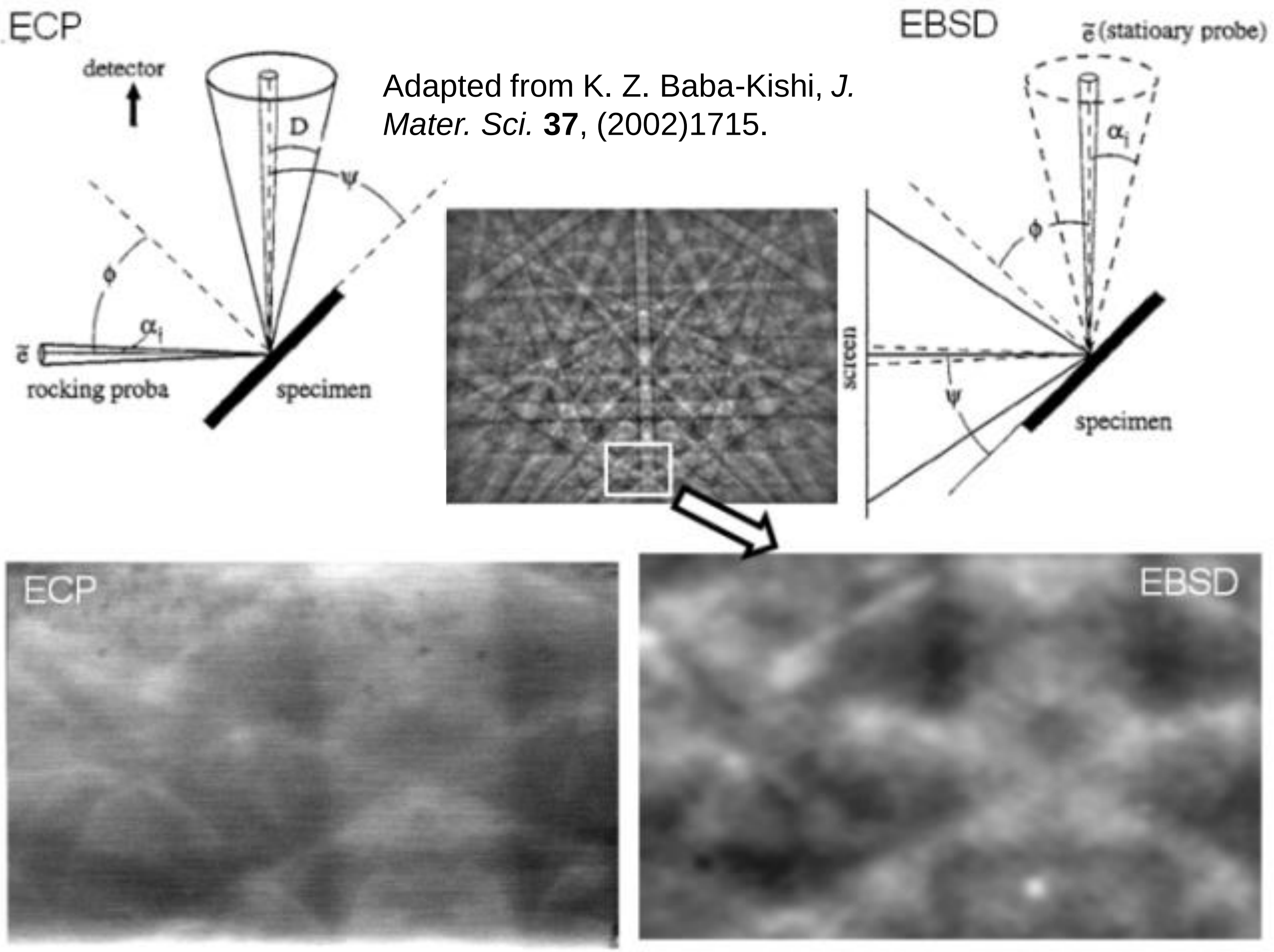

Adapted from K. Z. Baba-Kishi, *J. Mater. Sci.* **37**, (2002)1715.

Low Magnification BSE Image

Forescatter Geometry

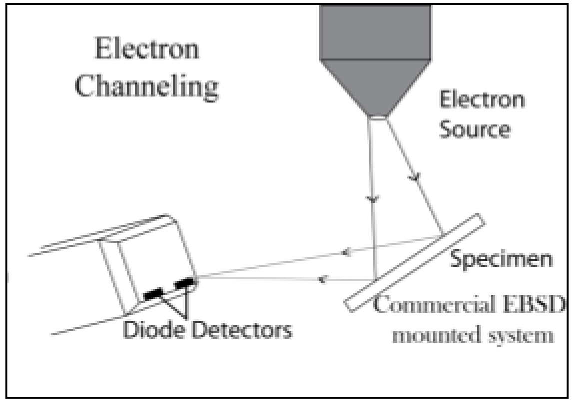

Backscatter Geometry

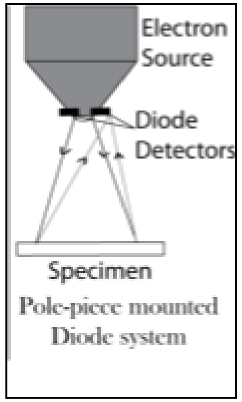

Yoosuf N. Picard, Materials Science & Engineering

Electron Channeling Contrast Imaging

"It should in principle be possible to use the <u>scanning electron microscope to detect dislocations</u> by the direct examination of unetched crystal surfaces. It is only necessary to orientate the crystal at the Bragg position and the <u>local bending</u> of these crystallographic planes should produce the necessary contrast. Such contrast should be directional and <u>could lead to Burgers vector determination</u>."

G.R. Booker, AMB Shaw, M.J. Whelan and P.B. Hirch, Philosophical Magazine **16**, 1185 (1967).

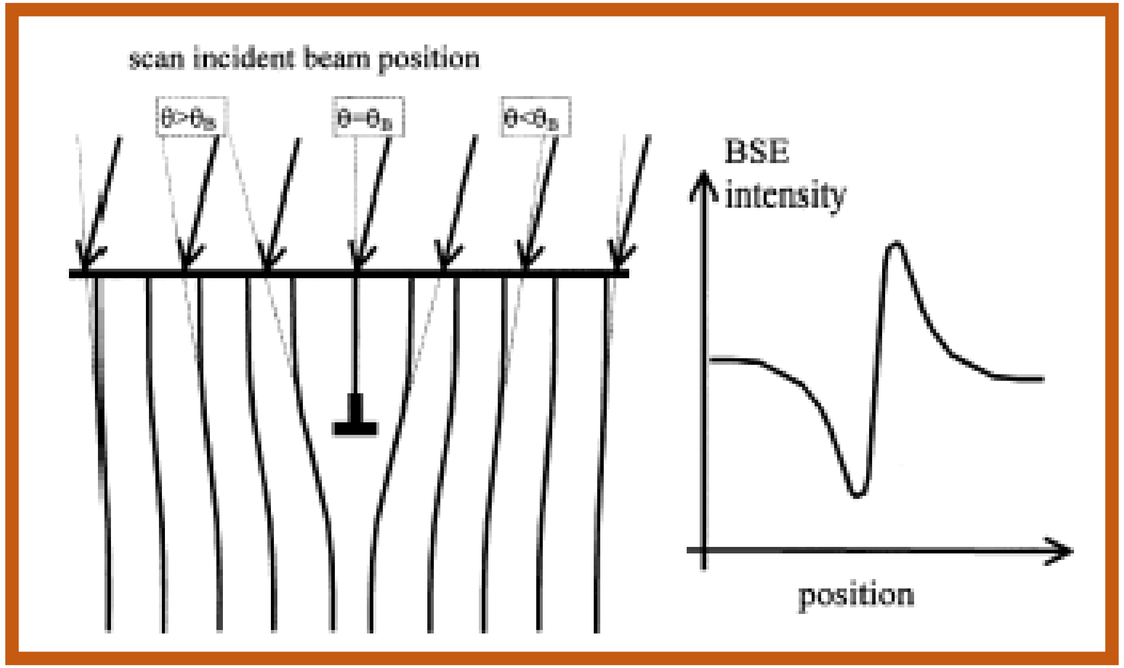

J. Ahmed *et al*, J. Microscopy **195**, 197 (1999).

Intensity fluctuation due to local lattice bending by dislocation

This is the basis for non-destructive defect imaging by ECCI

Previous ECCI Work

Si (111) - dislocations

ECCI

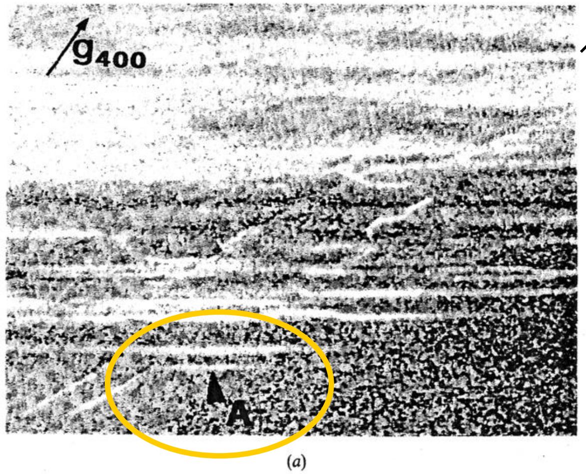

g_{400}

ECCI

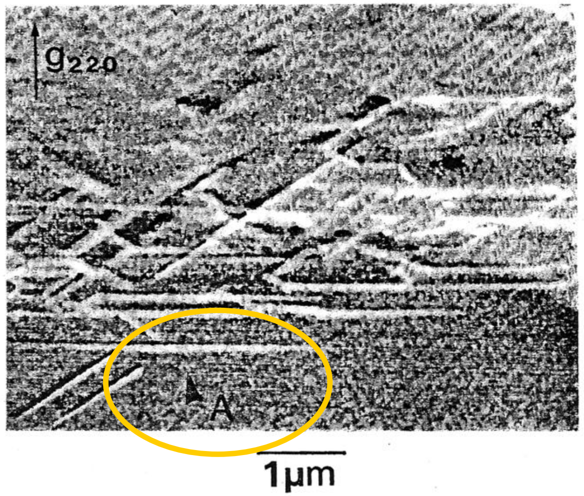

g_{220}

J.T. Czernuszka *et al*, Phil. Mag. Lett. **62**, 227 (1990).

Cu - Persistent slip bands (PSBs)

TEM

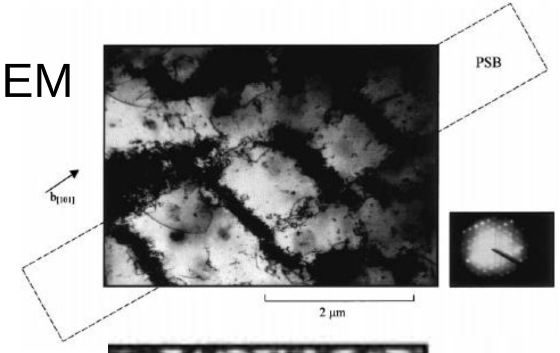

ECCI

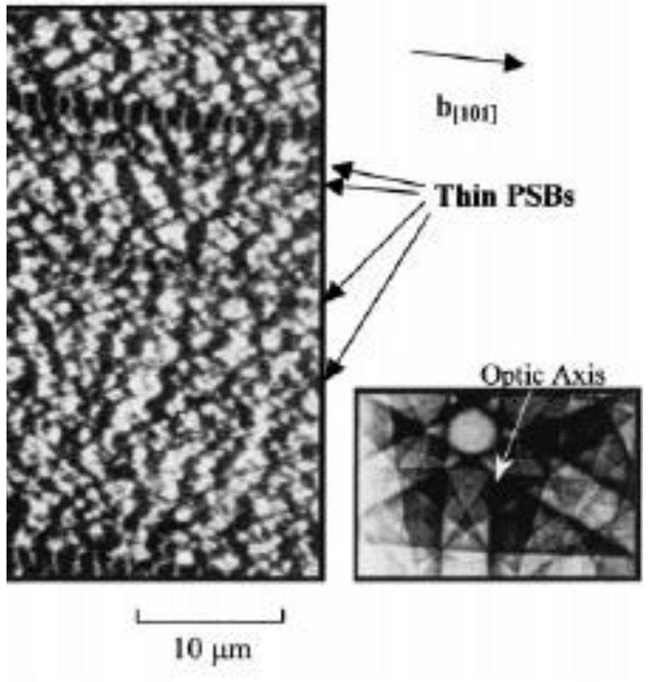

J. Ahmed *et al*, J. Microscopy **195**, 197 (1999).

More Recent ECCI Results

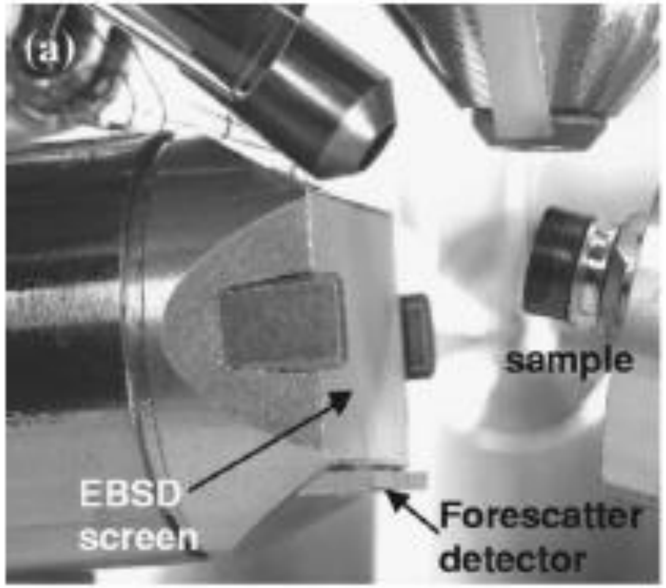

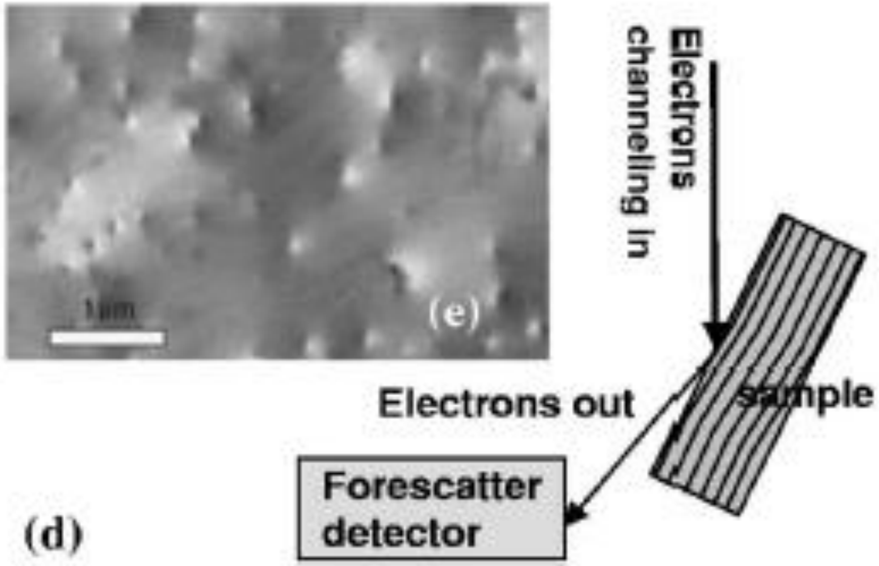

MOVPE GaN film on sapphire

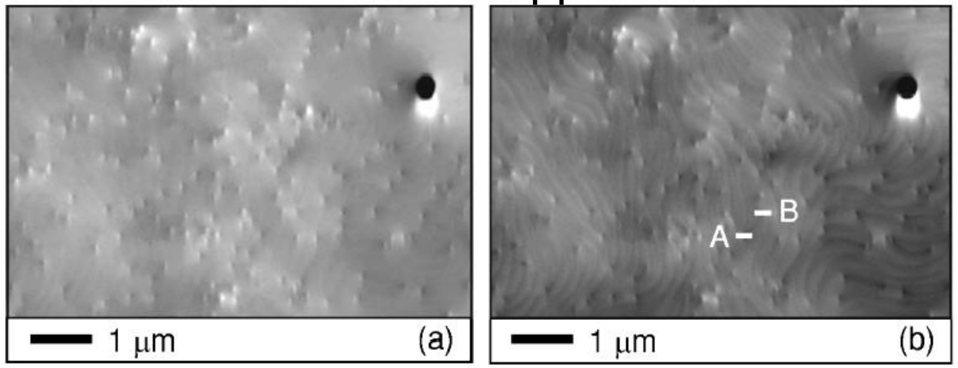

Individual dislocations can be imaged in an SEM

Atomic steps visible

C. Trager-Cowan *et al*, Phys. Rev. B. **75**, 085301 (2007).

Channeling vs. Conventional SEM

Backscatter Electron Detection – On Diffraction Condition

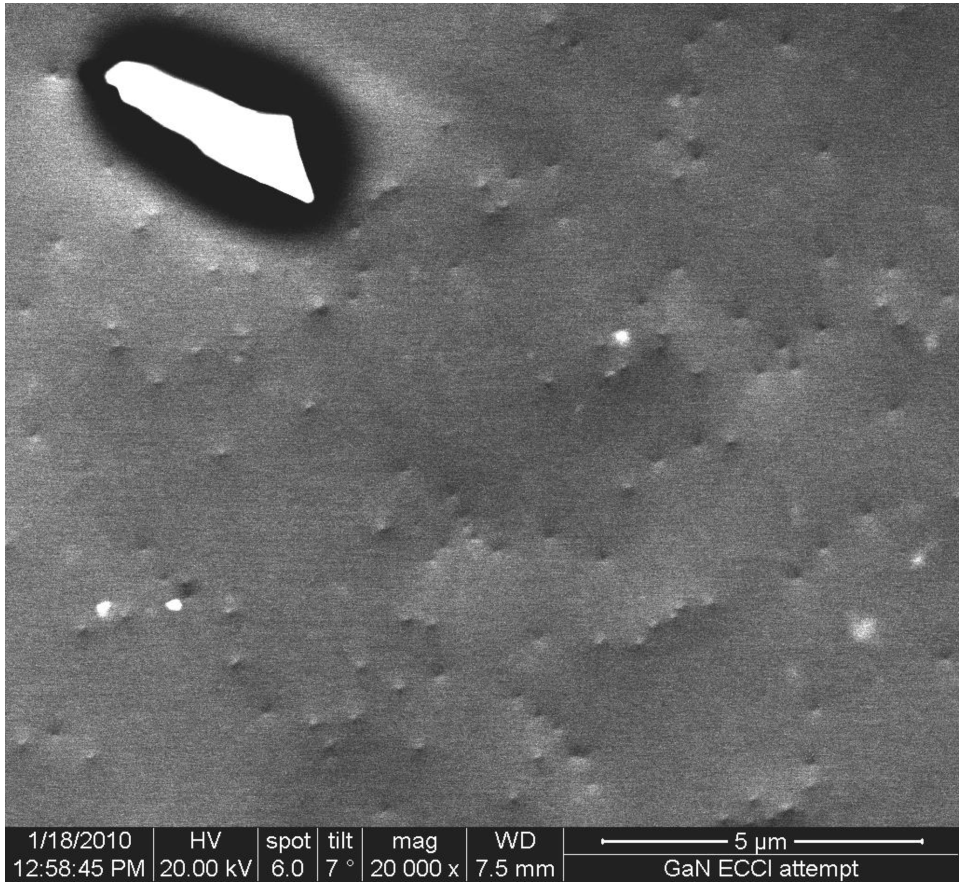

Secondary Electron Detection – Conventional SEM

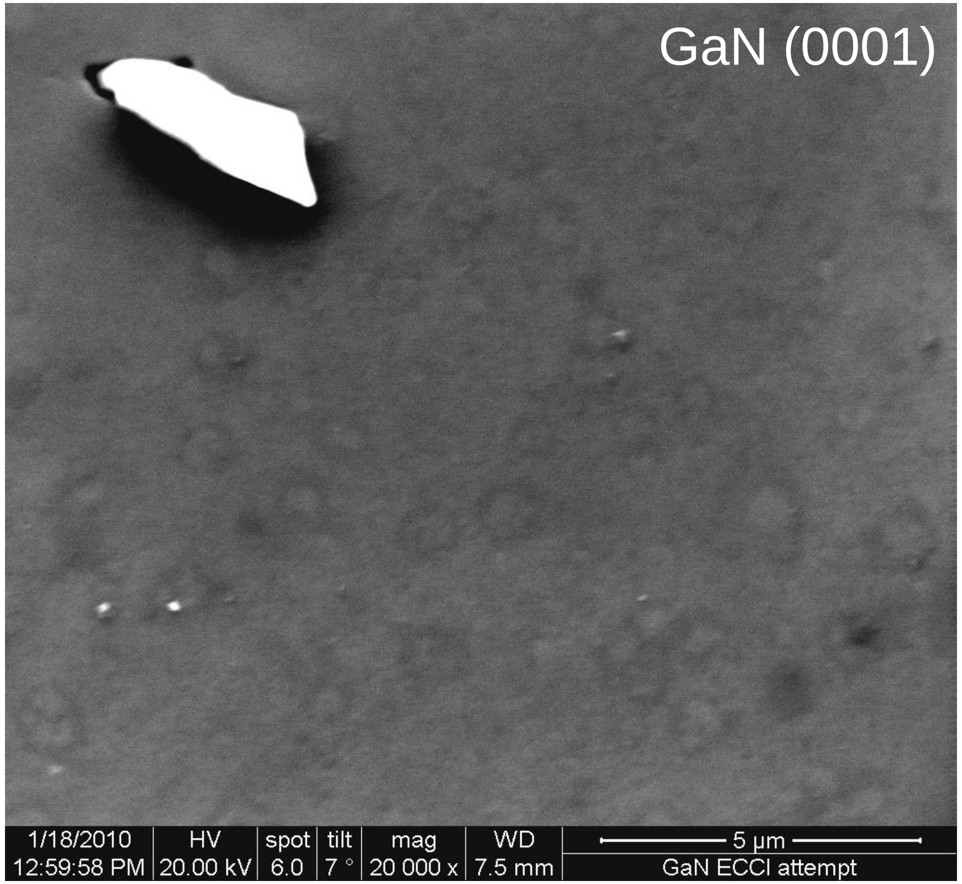

Two Geometries

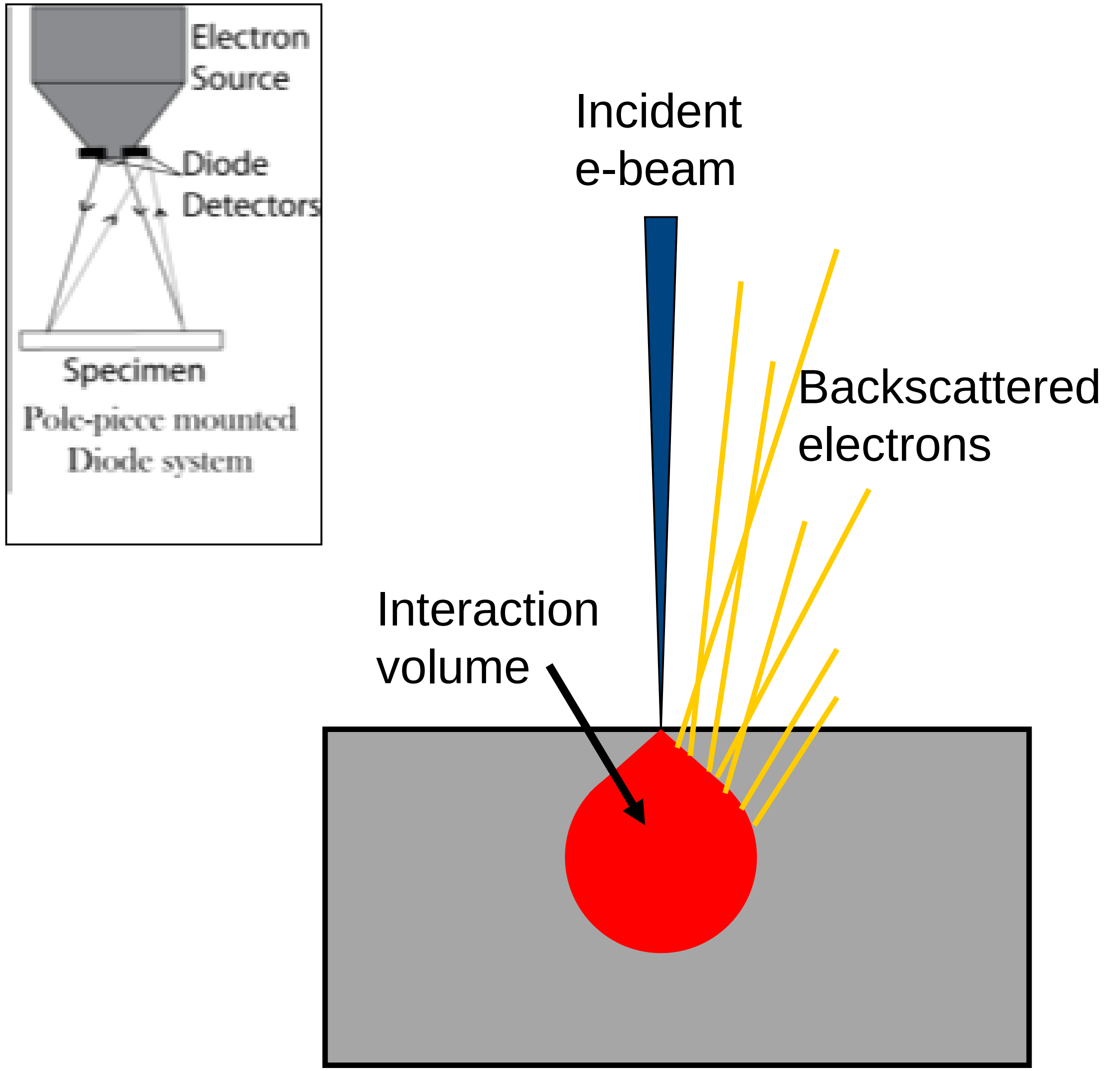

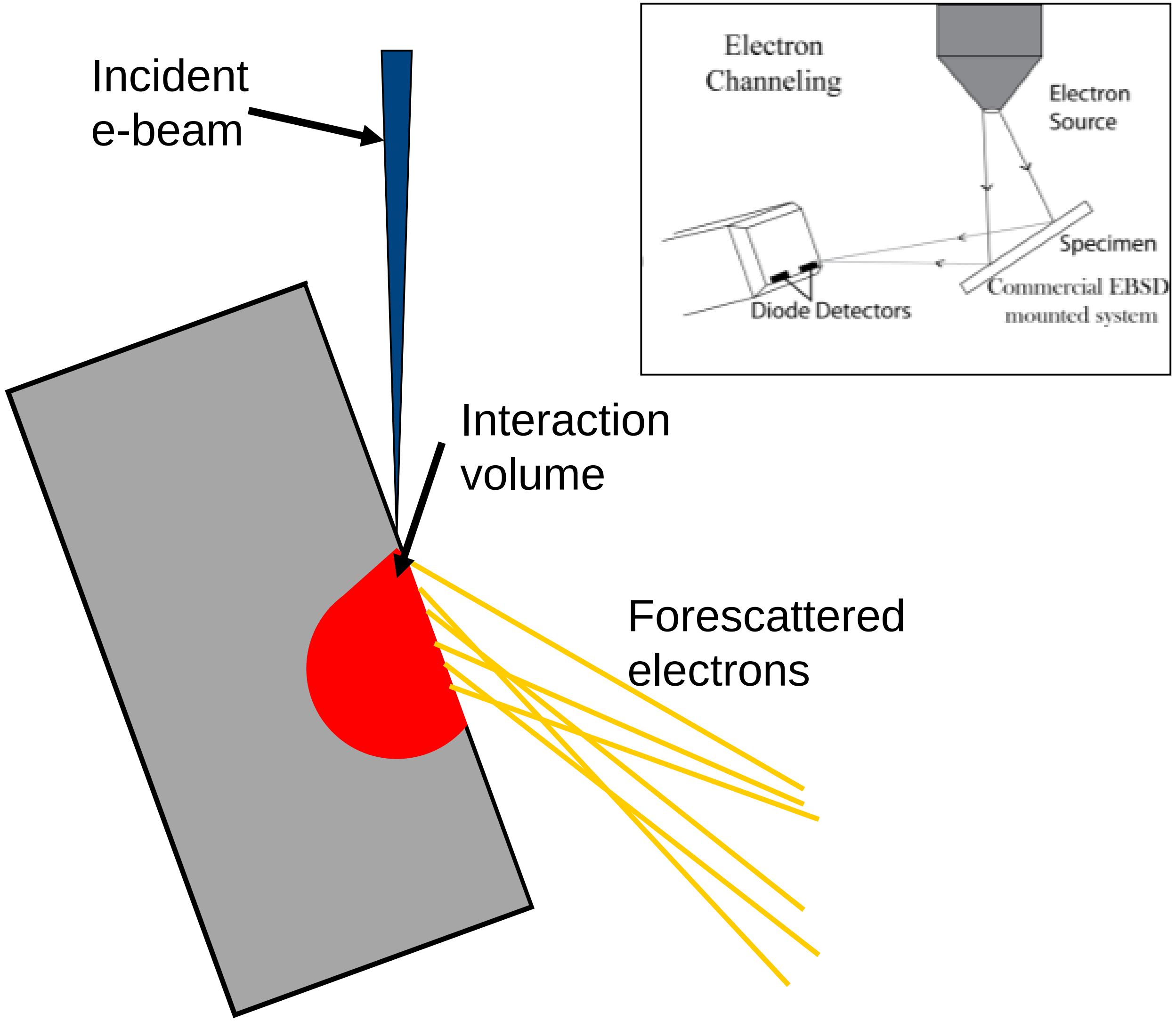

Example Experimental Approaches

Forescatter Geometry

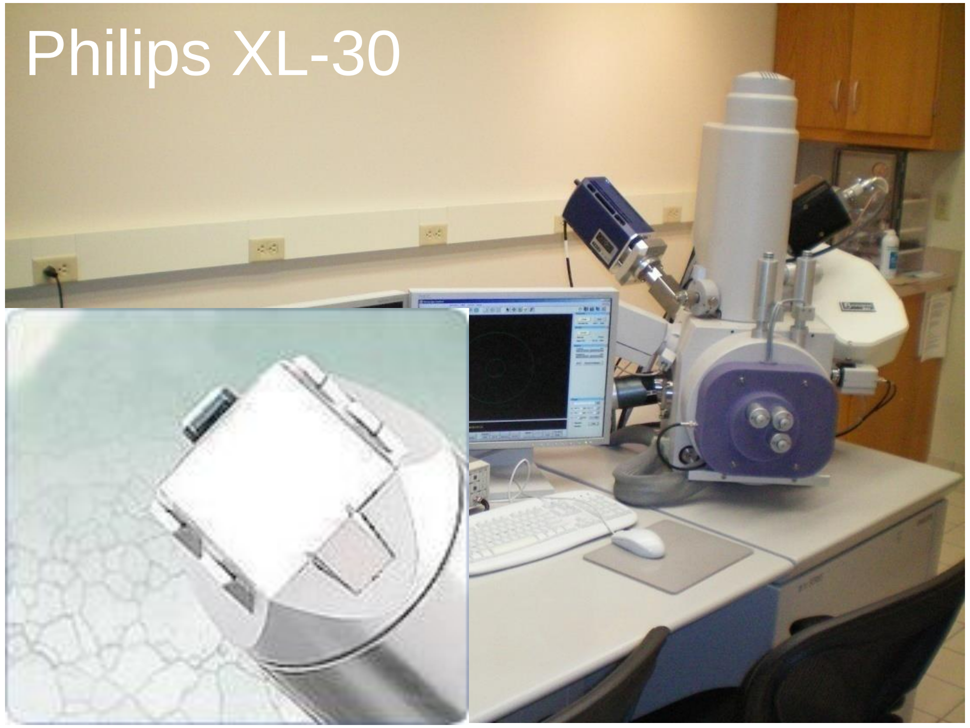

Courtesy of Oxford Instruments

Backscatter Geometry

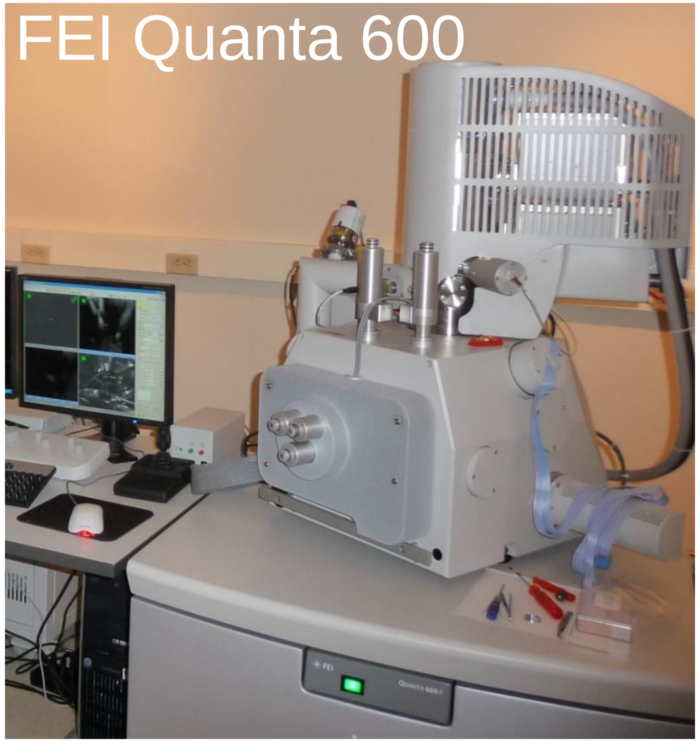

Forescatter diodes on EBSD
10-30 kV, 4-6 spot size
Samples tilted 50-70°

nA's of current

Annulus BSE detector
10-30 kV, 5-6.5 spot size
Samples tilted 5-20°

Modern ECCI Approach

1. BSE Image Single Crystal at Lowest Magnification

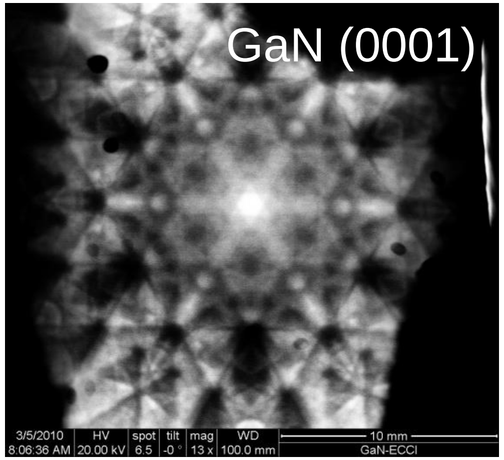

2. Use Resultant ECP to Orient Sample (Tilt/Rotate)

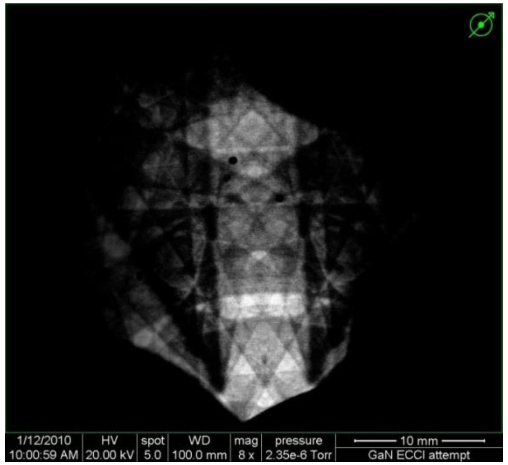

3. Magnify to Sample Surface

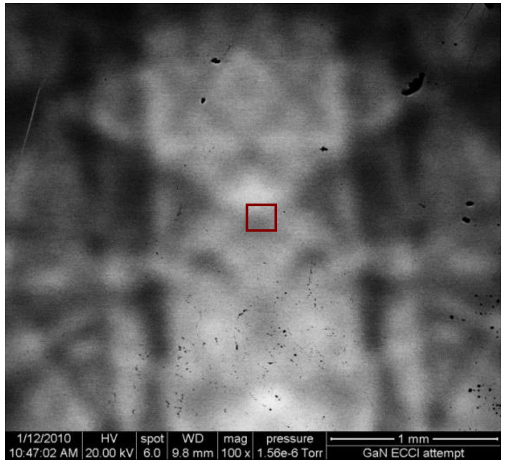

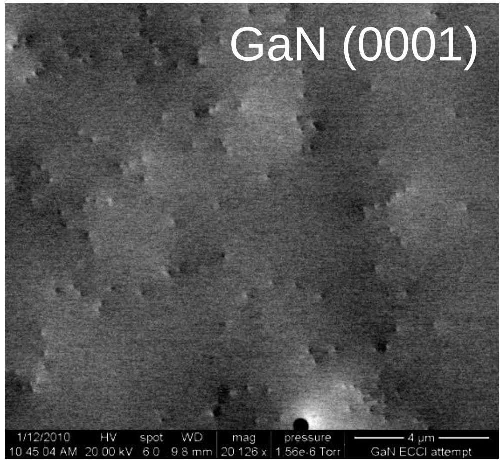

M. A. Crimp, “Scanning electron microscopy imaging of dislocations in bulk materials, using electron channeling contrast.” **Microsc. Res. Tech. 69**, 374 (2006).

R.J. Kamaladasa, Y.N. Picard, “Basic principles and application of electron channeling in a scanning electron microscope for dislocation analysis” **Microscopy: Science, Technology, Education and Applications. Vol. 4**, 1583 (2011).

ECCI Methods – Important Points

1. Channeling signal is much weaker than topographic and Z-contrast information in BSE image

2. Detector-sample positioning (working distance) needs to be optimized to maximize BSE collection

3. Detector gain settings (brightness/contrast/gamma) will need adjusting to maximize channeling BSE contrast

Single Screw Dislocation (4H-SiC)

Secondary Electron Image

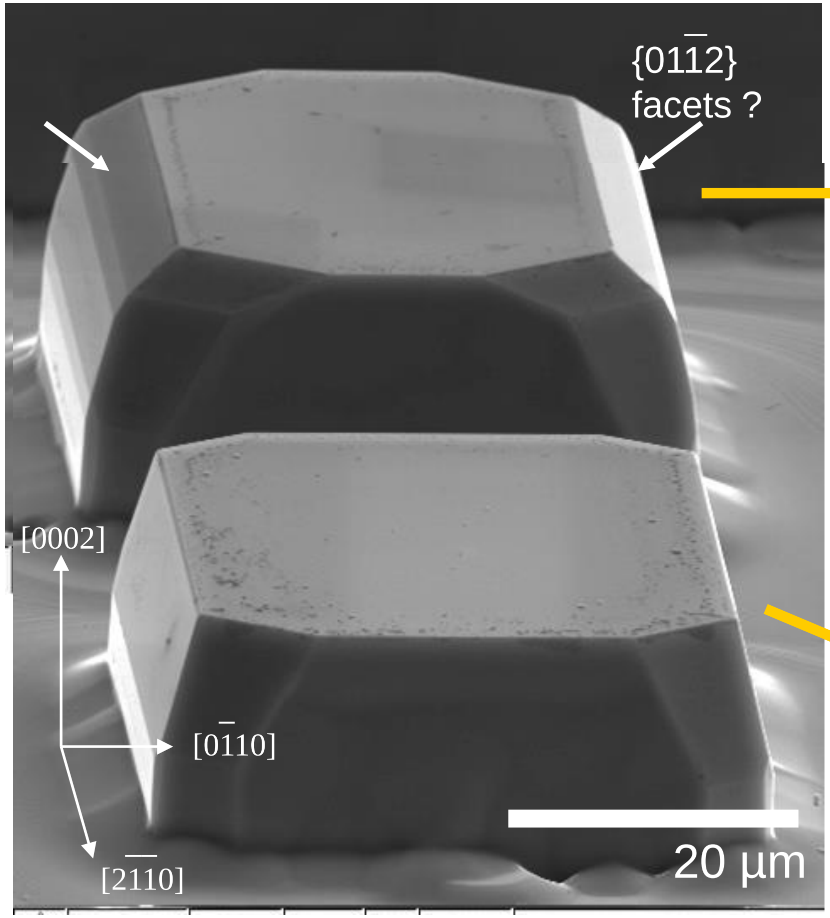

Vertical growth: Top Mesa > Bottom Mesa?

Y.N. Picard *et al*, Appl. Phys. Lett. **90**, 234101 (2007).

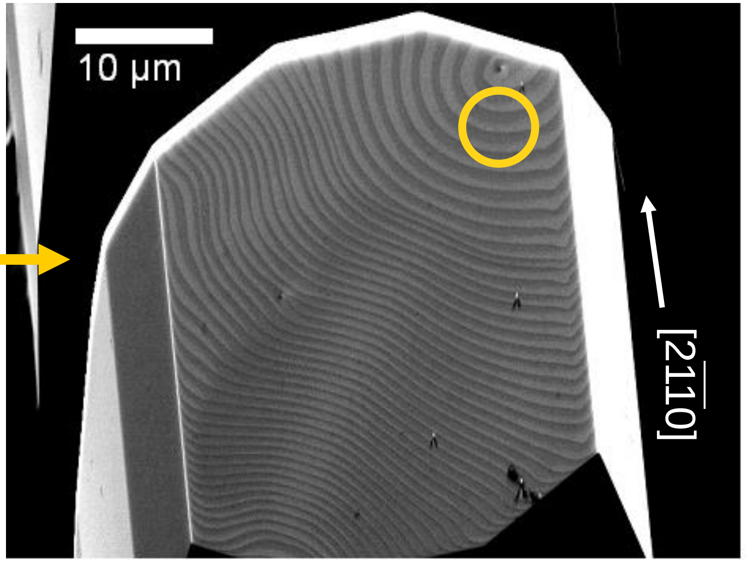

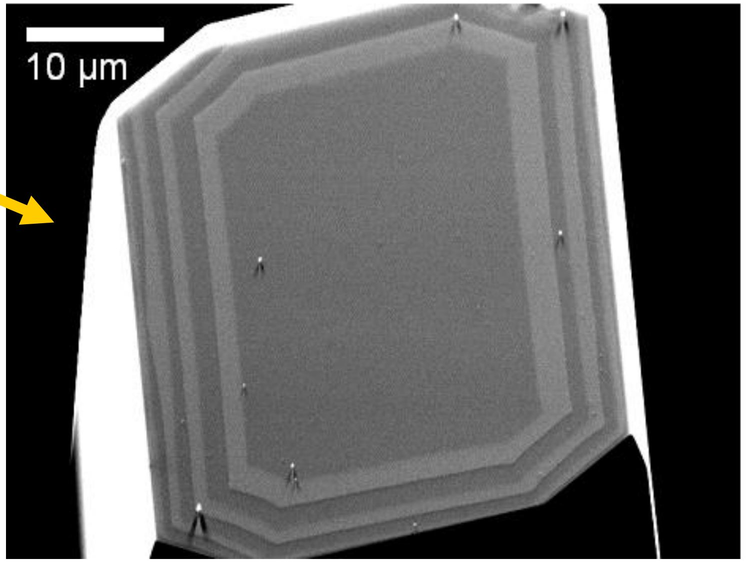

Forescattered Electron Images

Atomic Step morphology centers about screw dislocations

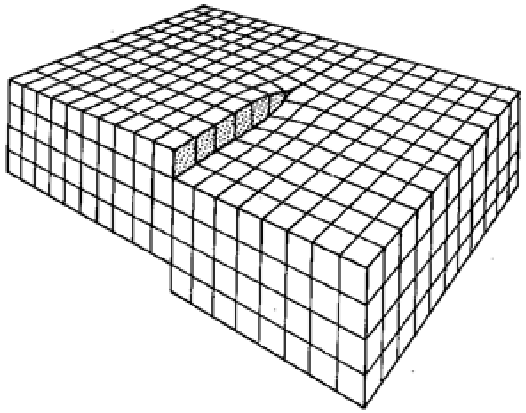

Single Screw Dislocation = Intensity Fluctuation

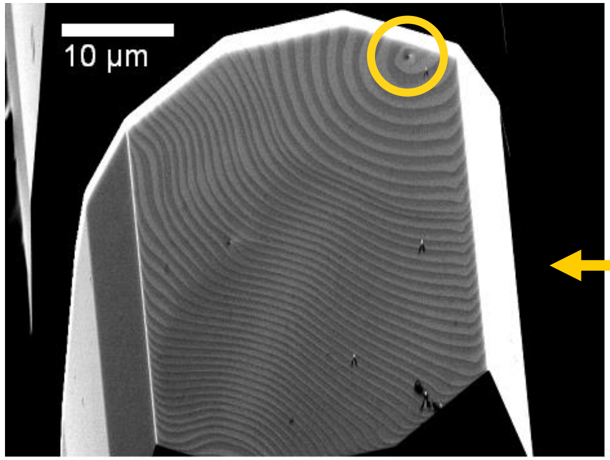

Electron Channeling Contrast Imaging (ECCI)

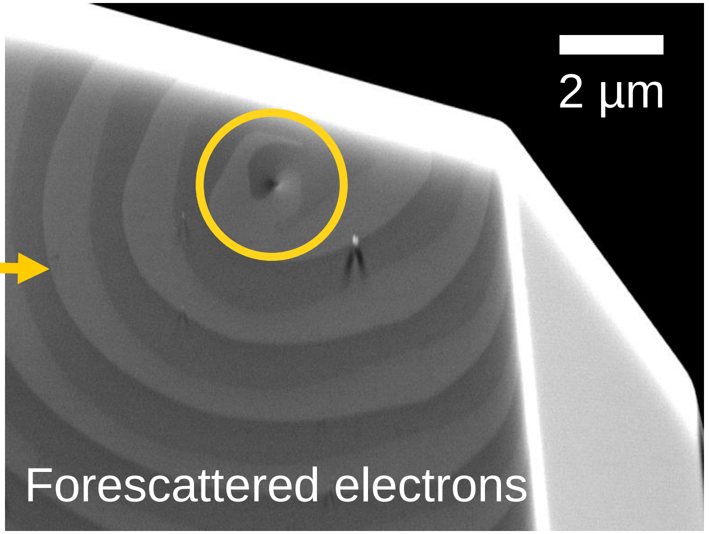

Intensity fluctuation → local lattice bending due to dislocation

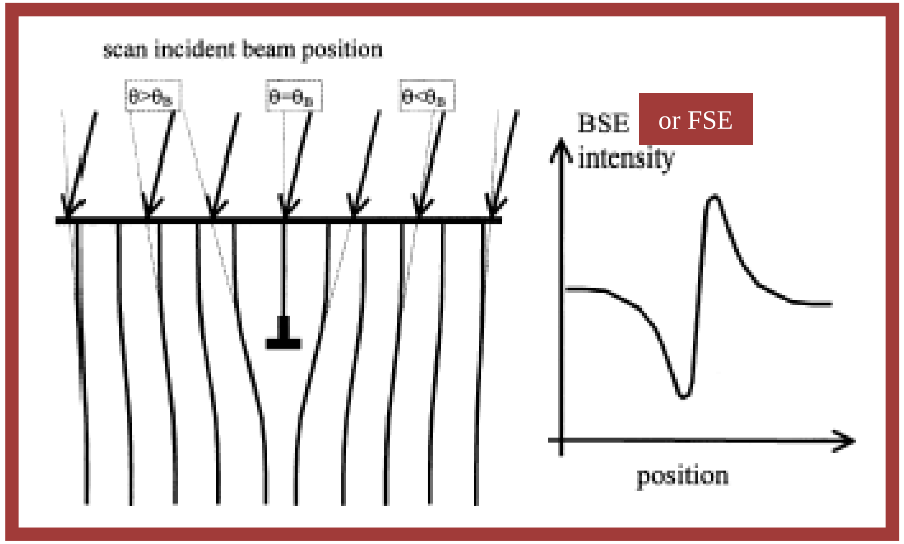

J. Ahmed *et al*, J. Microscopy **195**, 197 (1999).

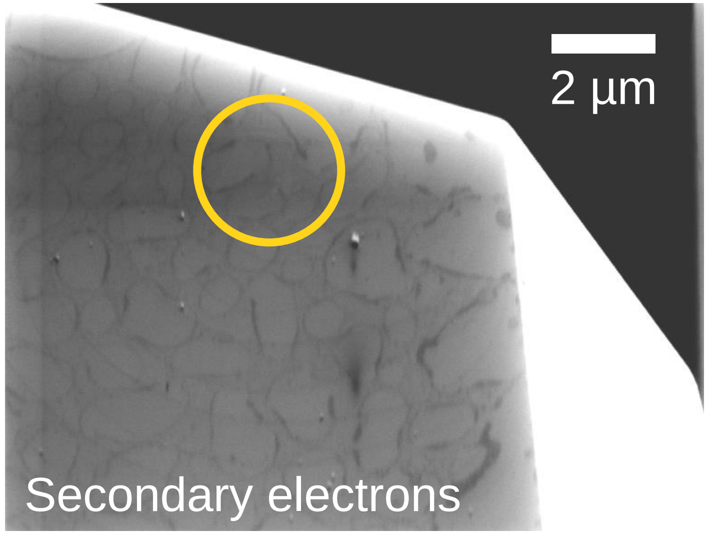

Y.N. Picard *et al*, Appl. Phys. Lett. **90**, 234101 (2007).

4H-SiC (0001)

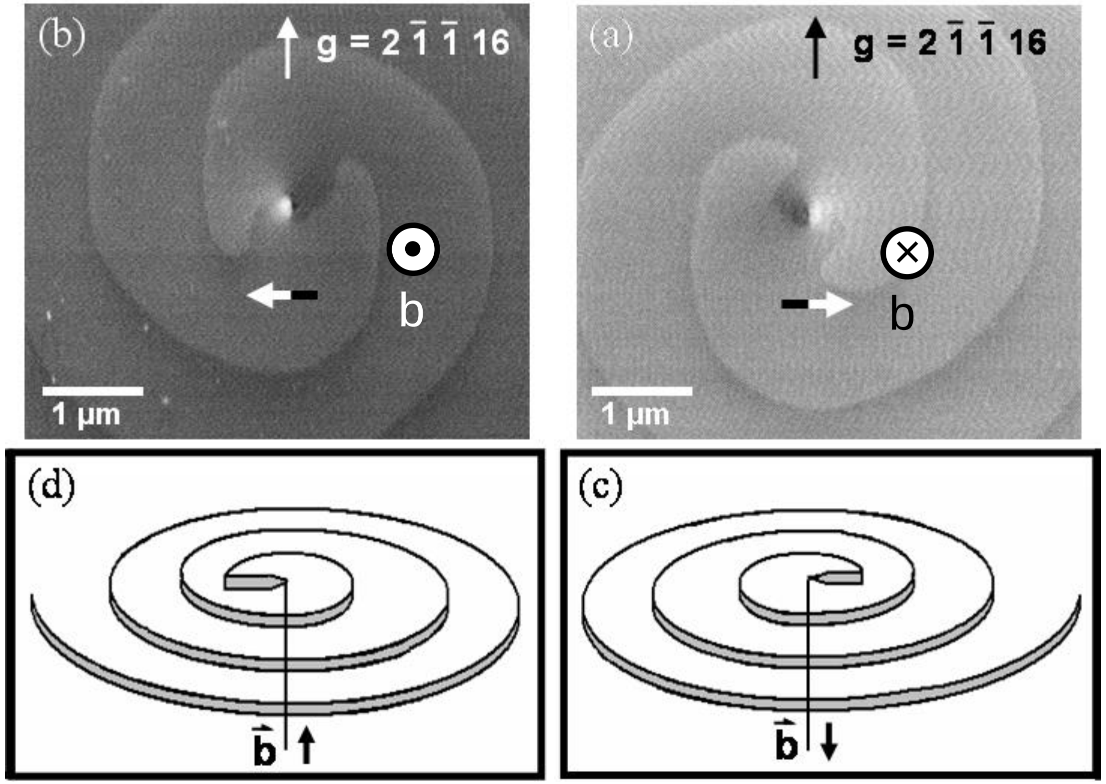

Y.N. Picard and M.E. Twigg, J. Appl. Phys. **104**, 124906 (2008).

Reversing Burgers vector, **b**, reverses the dark-to-light contrast

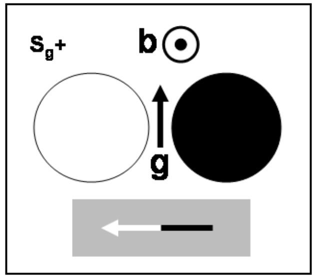

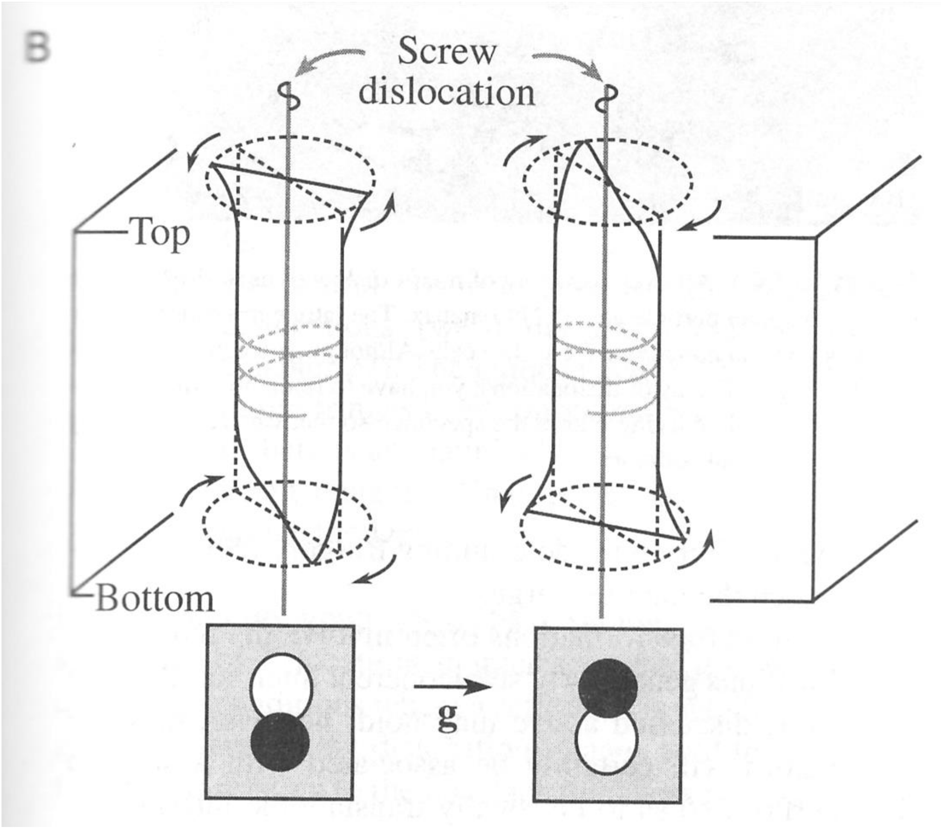

D.B. Williams and C.B. Carter, from p.415 of *Transmission Electron Microscopy*, Plenum Press, New York (1996).

ECCI of GaN

Threading dislocations = dark/light spots

atomic steps = lines

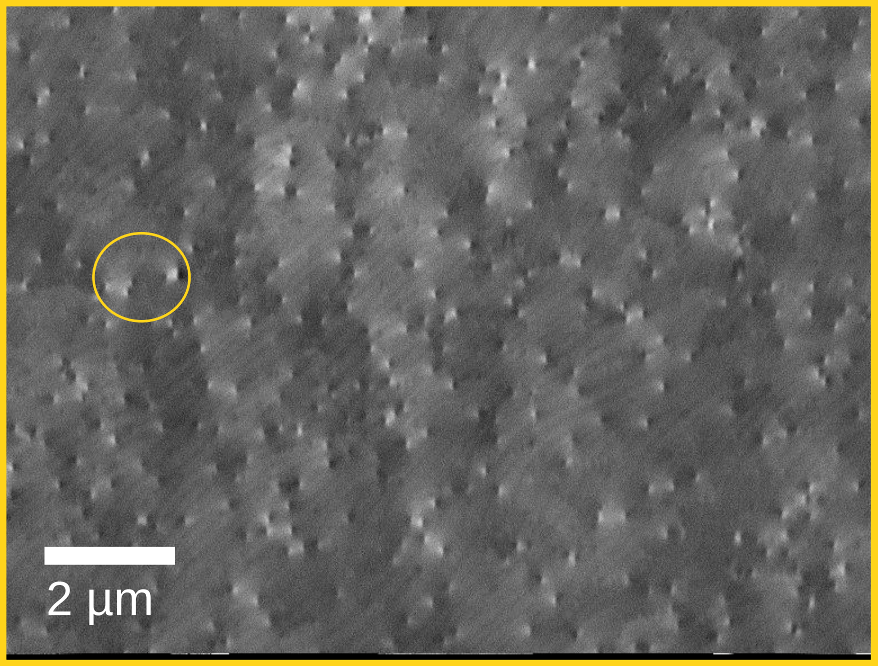

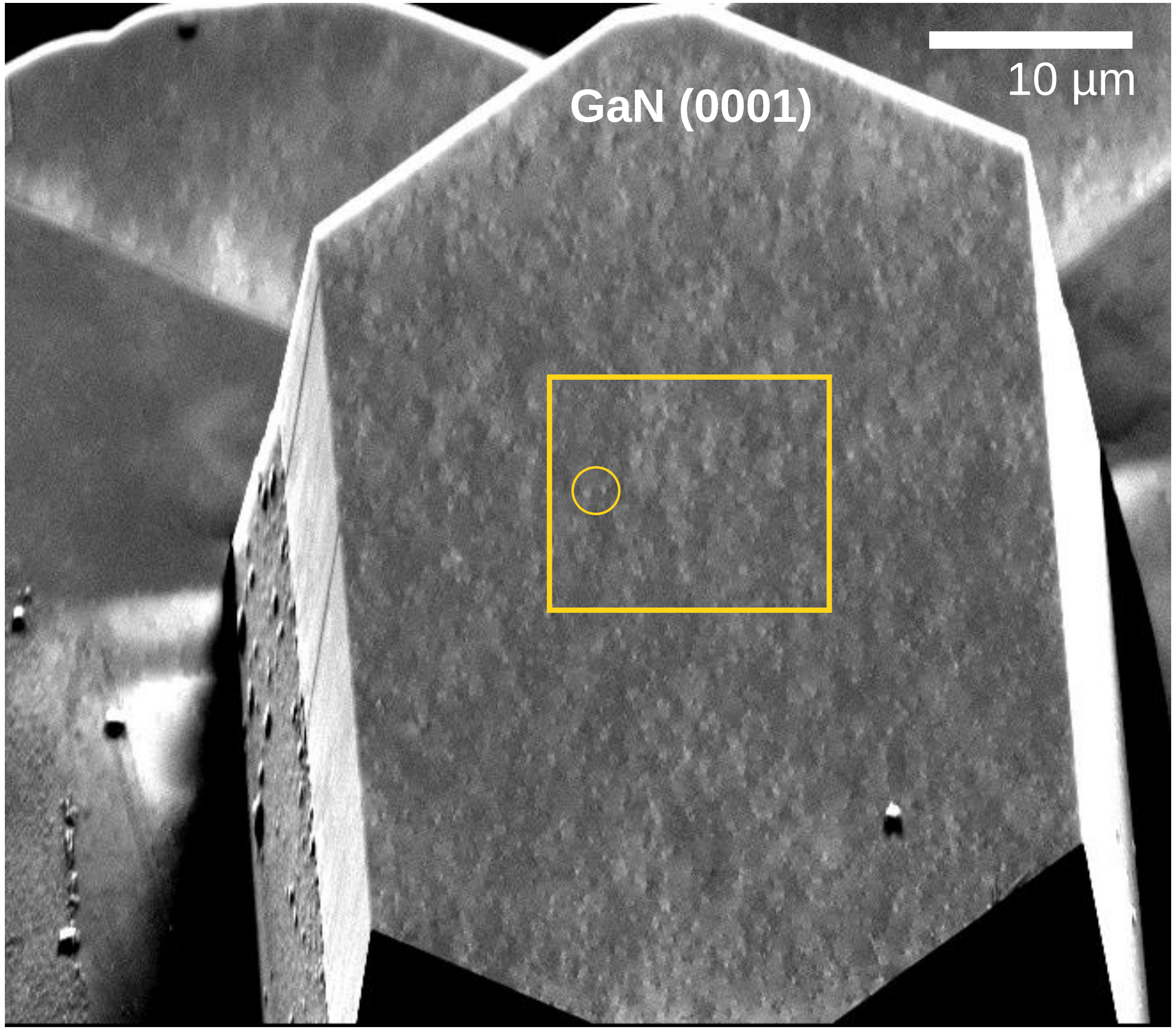

Defect imaging by ECCI resolvable over areas approaching 50 x 50 µm

Screw vs. Edge Delineation by ECCI

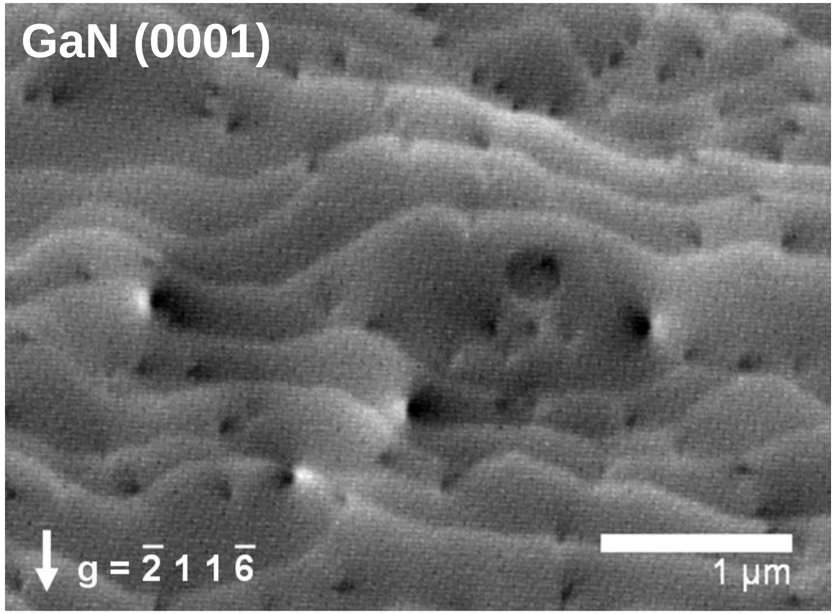

Two distinct intensity fluctuations:
Stronger and weaker

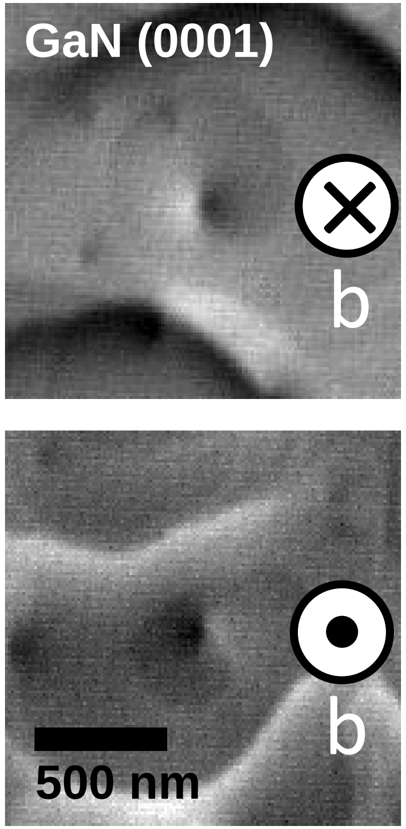

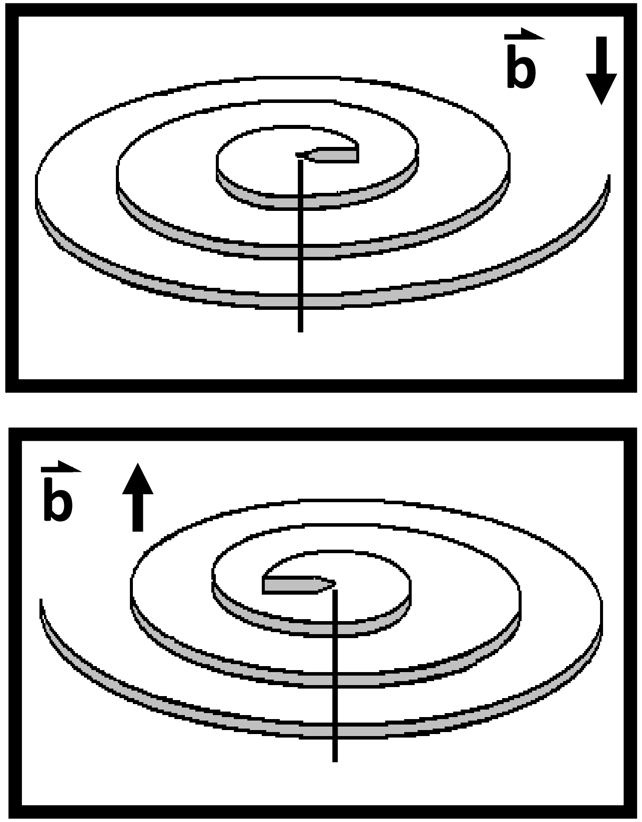

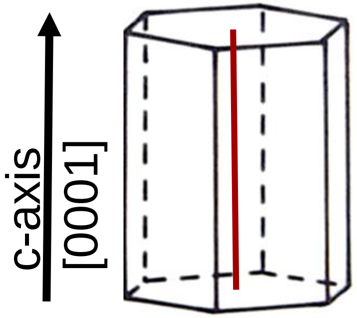

Screw > Edge

GaN
a = 3.189 Å
c = 5.185 Å

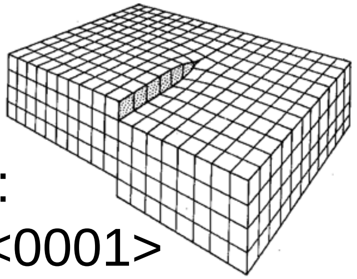

Screw:
b = c <0001>

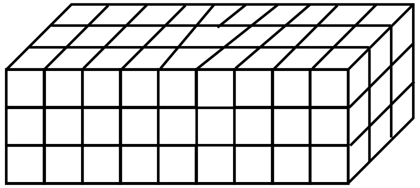

Edge: **b** = a/3 <11$\bar{2}$0>

Yoosuf N. Picard, Materials Science & Engineering
Carnegie Mellon

ECCI Validation – HVPE GaN Substrates

ECCI pre-etching **SEM post-etching**

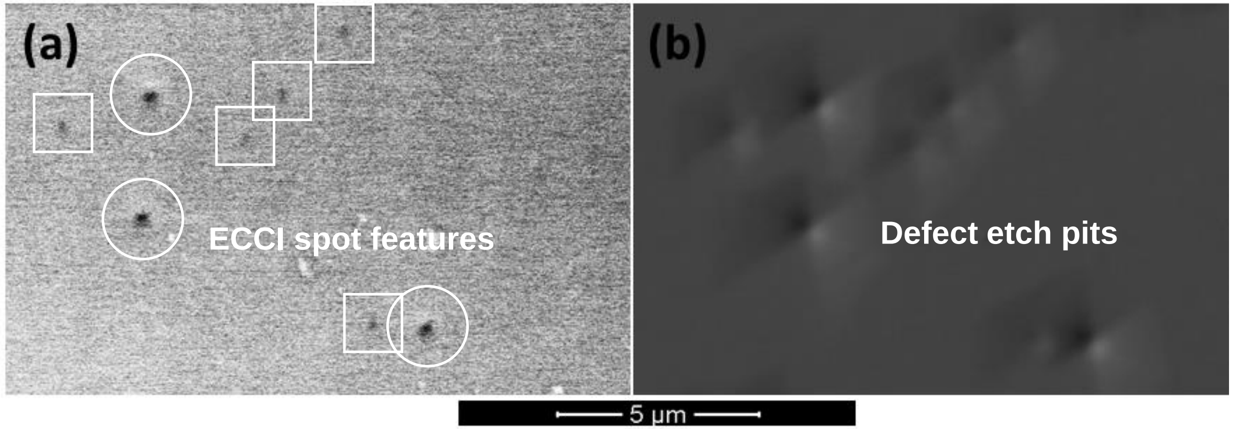

MgO:KOH etching confirms ECCI features are dislocations

Larger feature = Larger etch pit

TEM

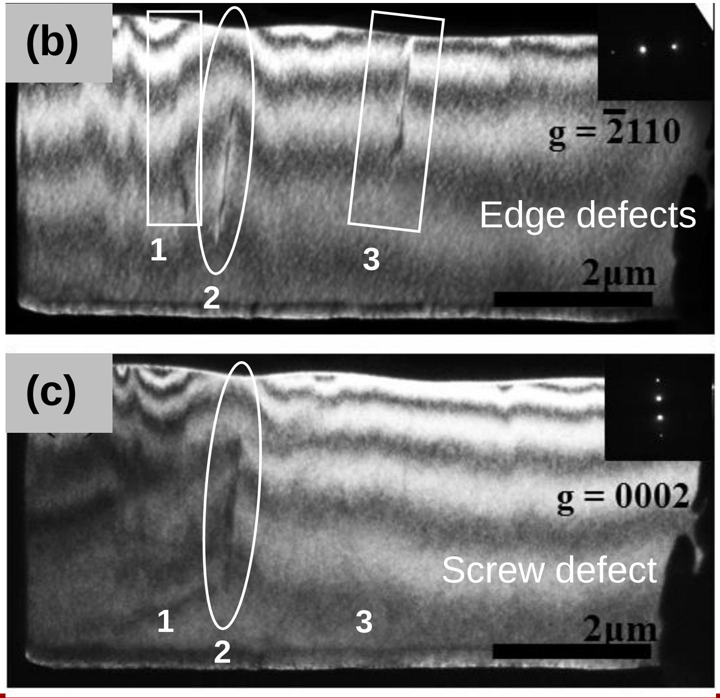

Site-specific TEM confirms differentiation between edge and mixed dislocations

Larger etch pit = Mixed dislocation

SEM post-etching

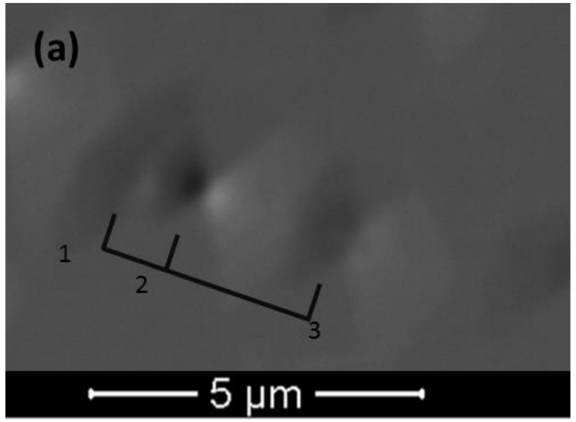

R.J. Kamaladasa et. al. **Journal of Microscopy, 244**(3), 311–319 (2011)

Edge Dislocations on Low-Angle Grain Boundaries

MOVPE GaN film on sapphire

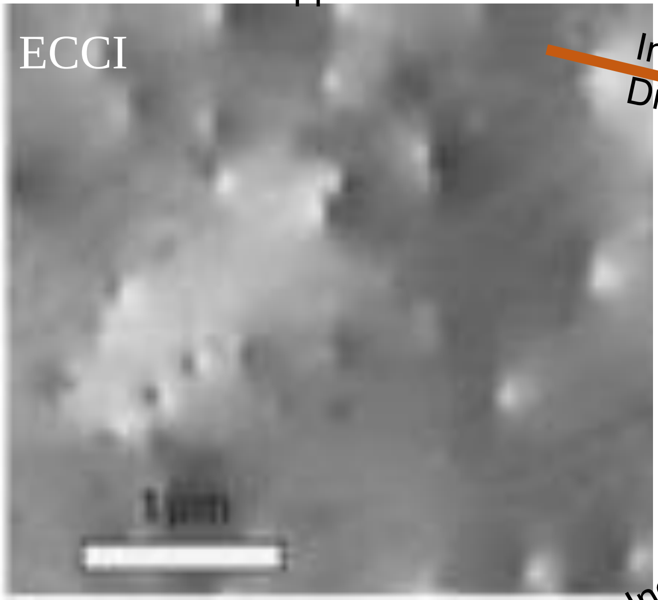

C. Trager-Cowan *et al*, Phys. Rev. B. **75**, 085301 (2007).

Individual Dislocations

Individual Grains

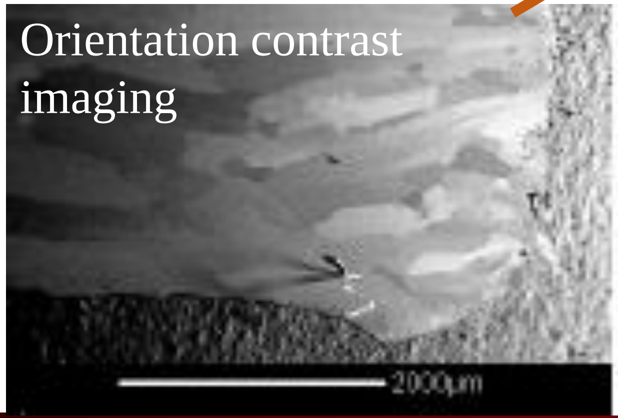

A. Day and P. Trimby, Channel 5 Instruction Manual, HKL Technologies, 2004.

MOCVD GaN (0001) film on 4H-SiC

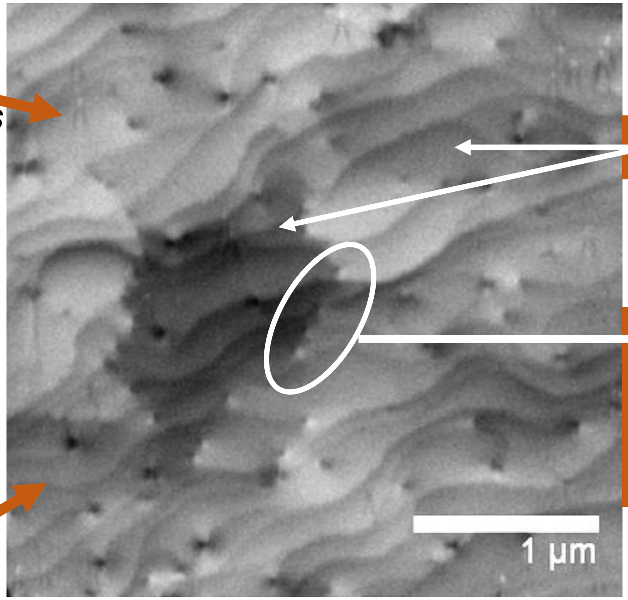

$\gamma = 25.1°; s_g = 0$

Individual "grains"

Threading dislocations along low-angle grain boundaries

Y.N. Picard *et al*, Appl. Phys. Lett. **91**, 094106 (2007).

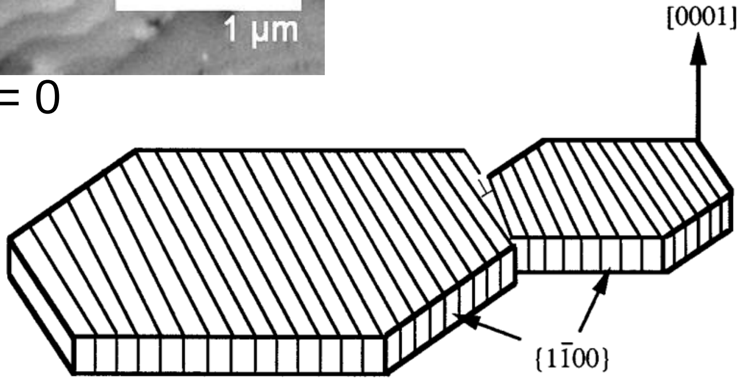

X.J. Ning *et al*, J. Mater. Res. **11**, 580 (1996).

ECCI technique sensitive to threading edge dislocations

Edge Dislocations on Low-Angle Grain Boundaries

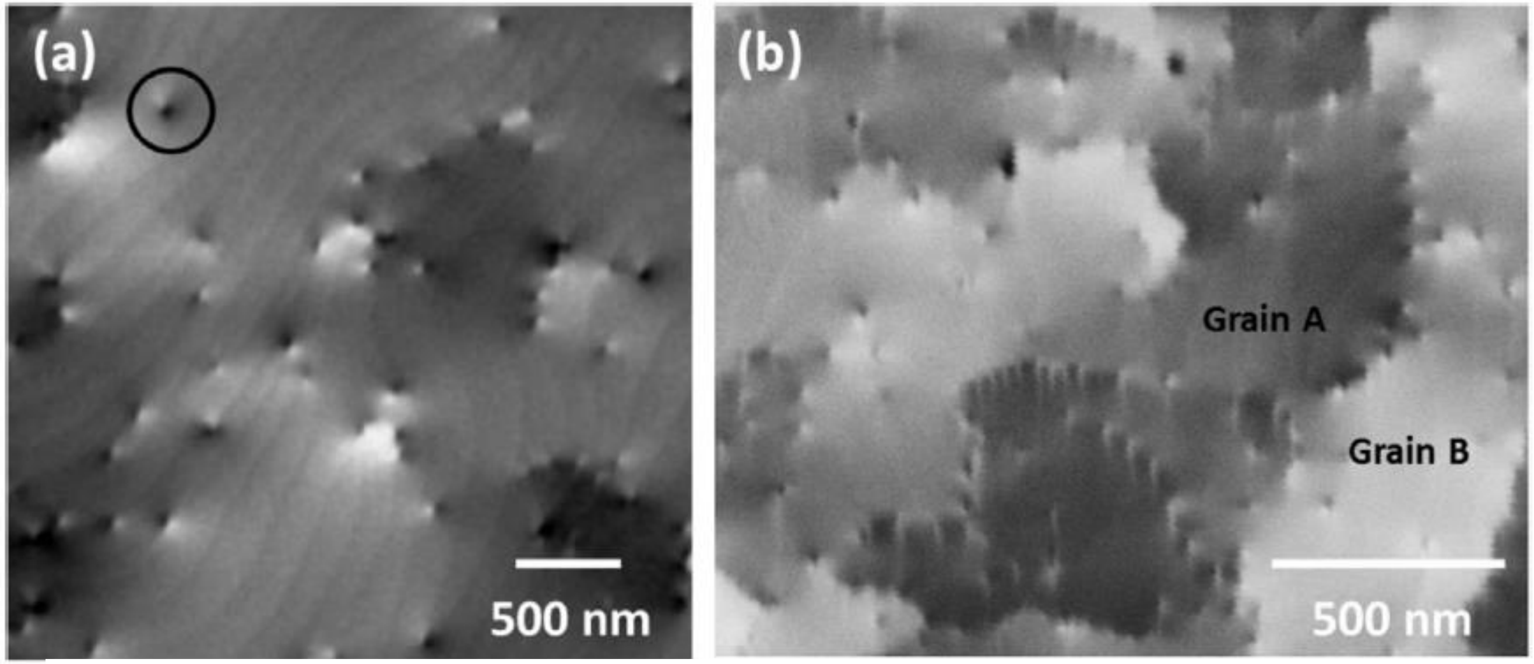

Materials Science in Semiconductor Processing 47 (2016) 44–50

Contents lists available at ScienceDirect

Materials Science in Semiconductor Processing

journal homepage: www.elsevier.com/locate/mssp

Electron channelling contrast imaging for III-nitride thin film structures

G. Naresh-Kumar*, D. Thomson, M. Nouf-Allehiani, J. Bruckbauer, P.R. Edwards, B. Hourahine, R.W. Martin, C. Trager-Cowan

Department of Physics, SUPA, University of Strathclyde, Glasgow G4 0NG, UK

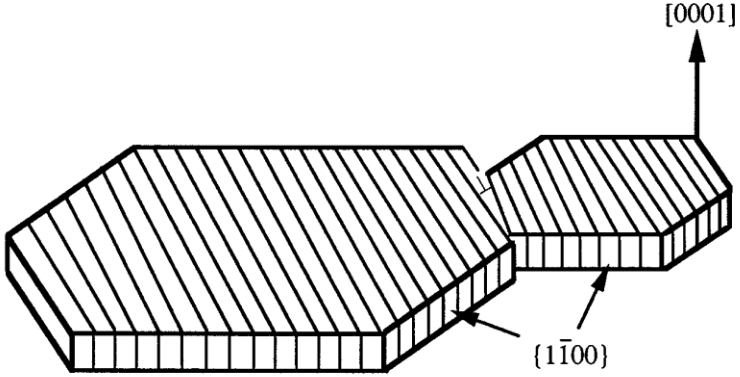

X.J. Ning *et al*, J. Mater. Res. **11**, 580 (1996).

ECCI technique sensitive to threading edge dislocations

Simulating Threading Dislocation Contrast

GaN (0001)

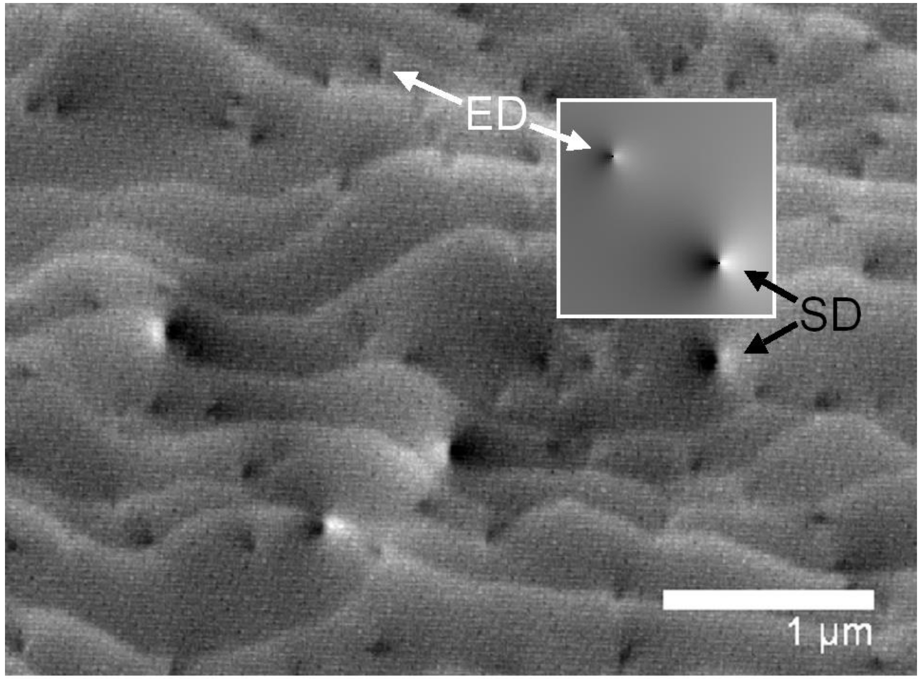

Resolving dislocation type

M.E. Twigg and Y.N. Picard. J. Appl. Phys. **105**, 093520 (2009).
Y.N. Picard *et. al.* Scripta Mater. **61**, 773 (2009).

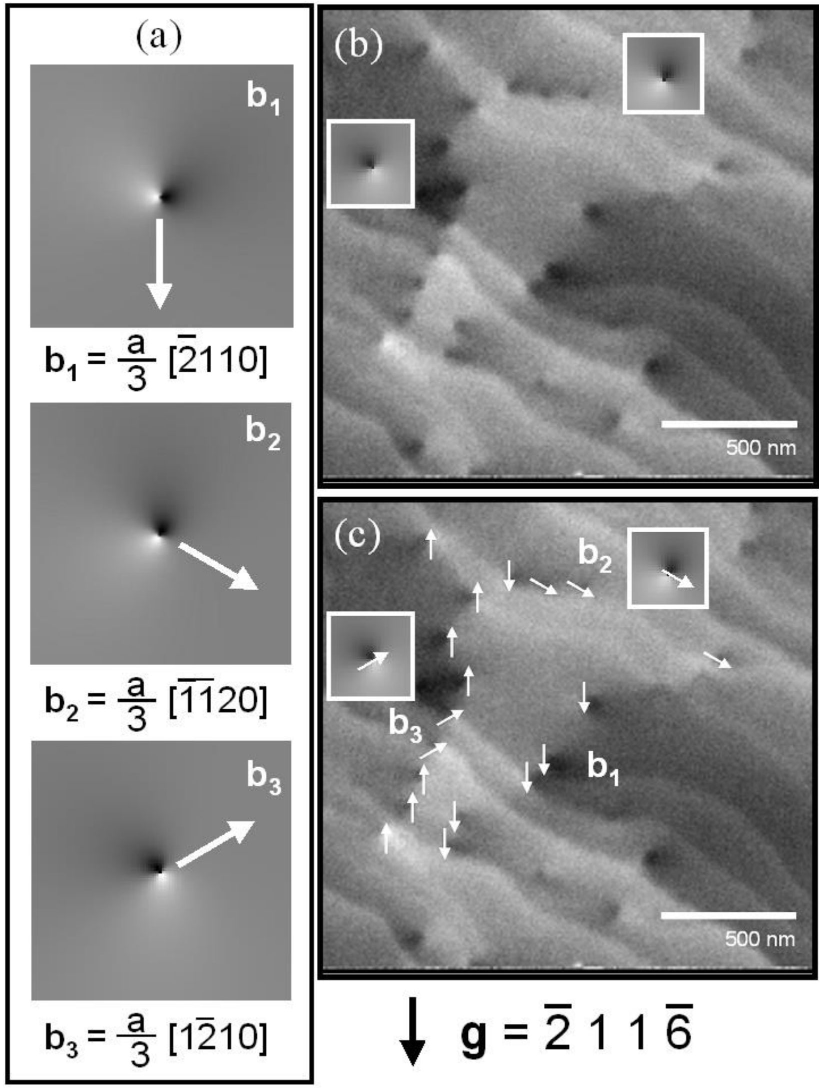

Resolving edge dislocation directionality

Comparing ECCI Geometries

Forescatter ECCI

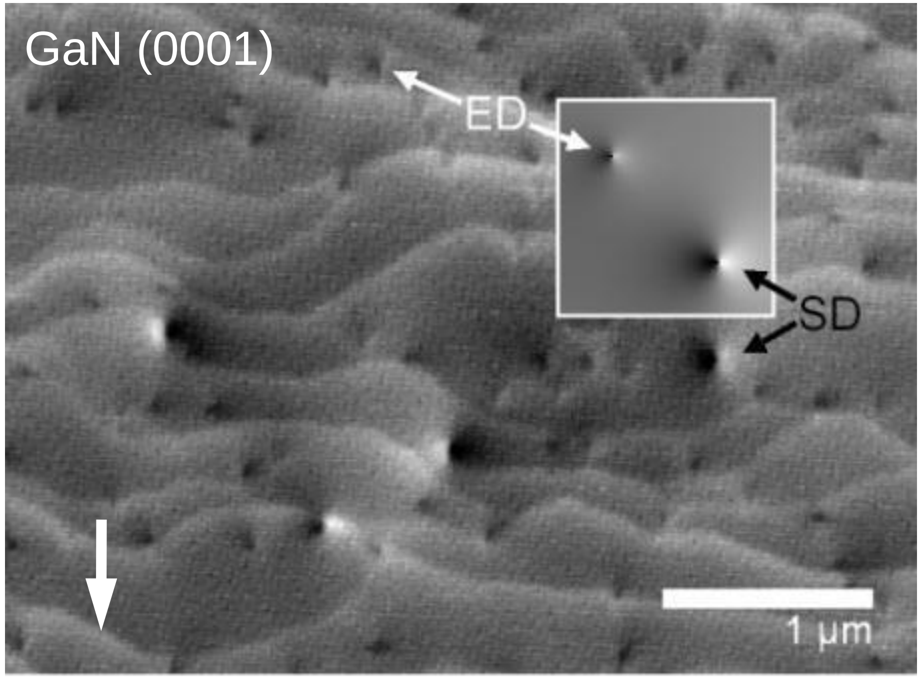

Y.N. Picard *et. al.* Scripta Mater. **61**, 773 (2009).

Backscatter ECCI

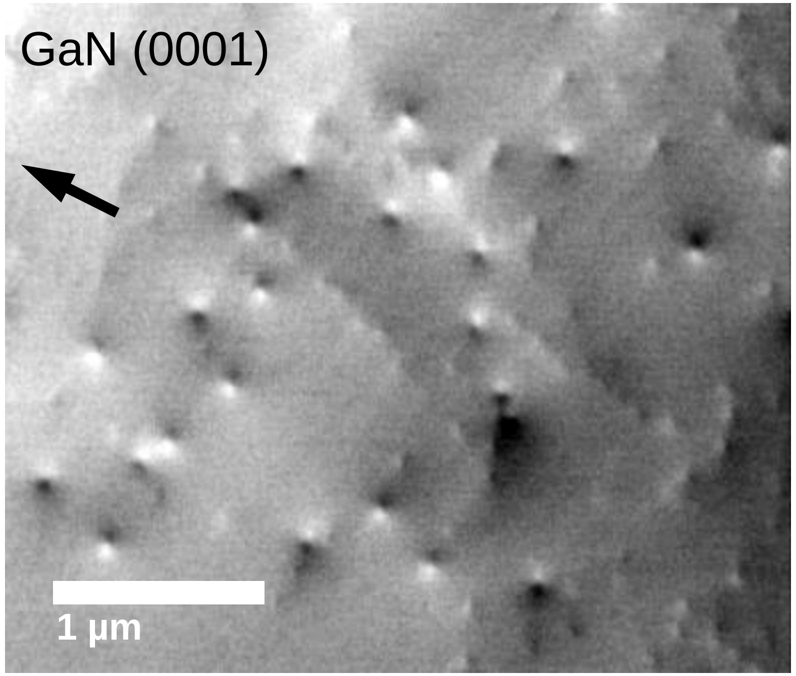

Surface distortion: Screw dislocation > Edge dislocation

Contrast Dependent on Diffraction Vector

GaN (0001): Rotating diffraction vector, **g**, rotates dark-light contrast features

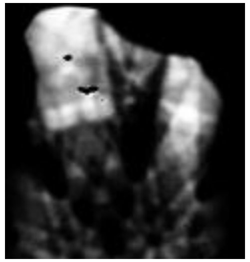

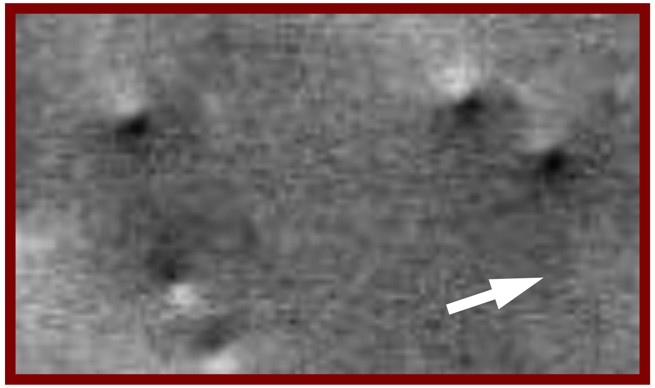

g = $[10\bar{1}0]$

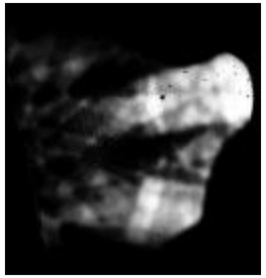

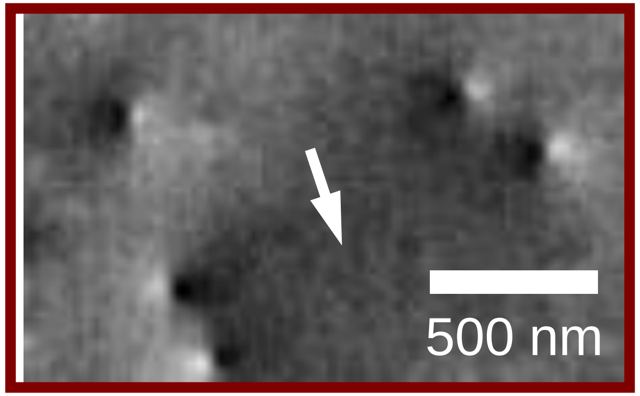

g = $[\bar{1}210]$

Y.N. Picard et. al. **Microscopy Today**. **20** (2), 12-16 (2012).

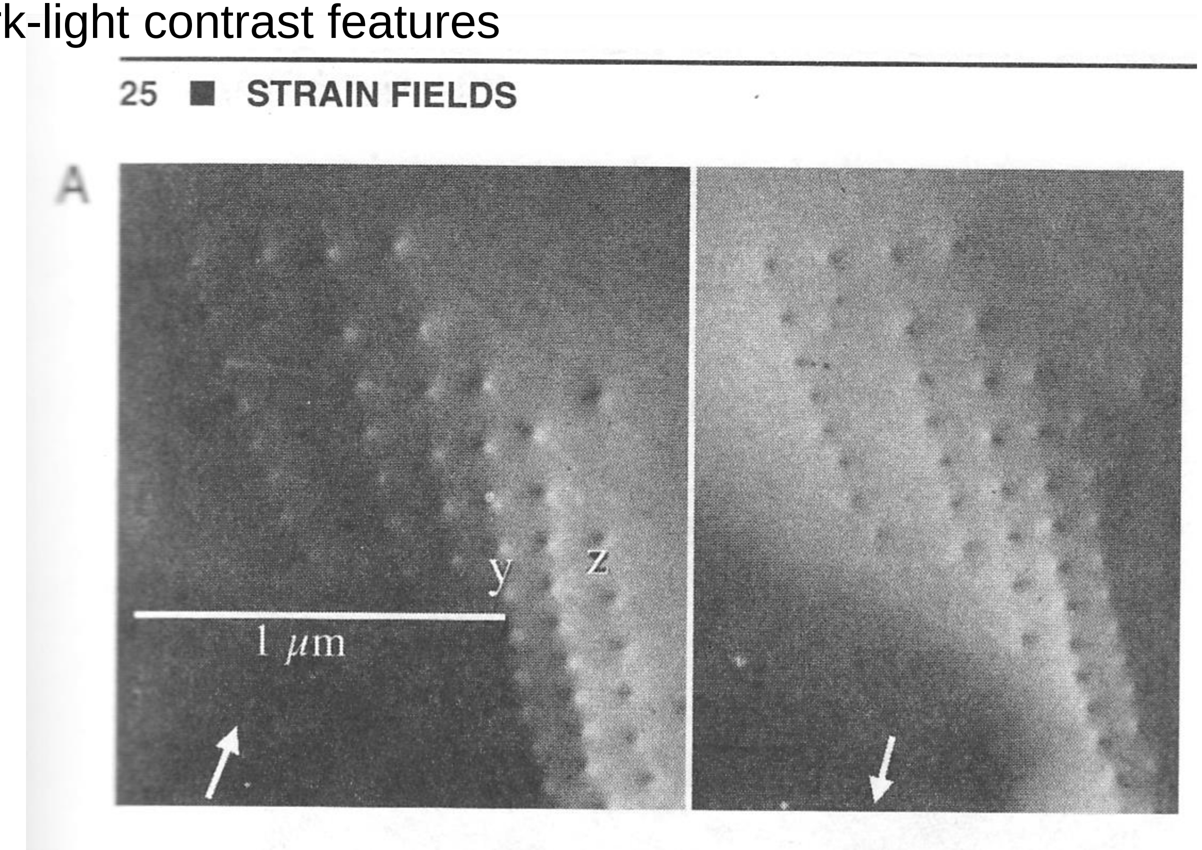

W.J. Tunstall et. al. Phil. Mag. **9**, 99 (1964). (as taken from D.B. Williams and C.B. Carter, p.415 of *Transmission Electron Microscopy*, Plenum Press, New York (1996).)

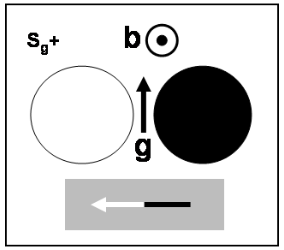

Dislocation Channeling Contrast – Line Direction

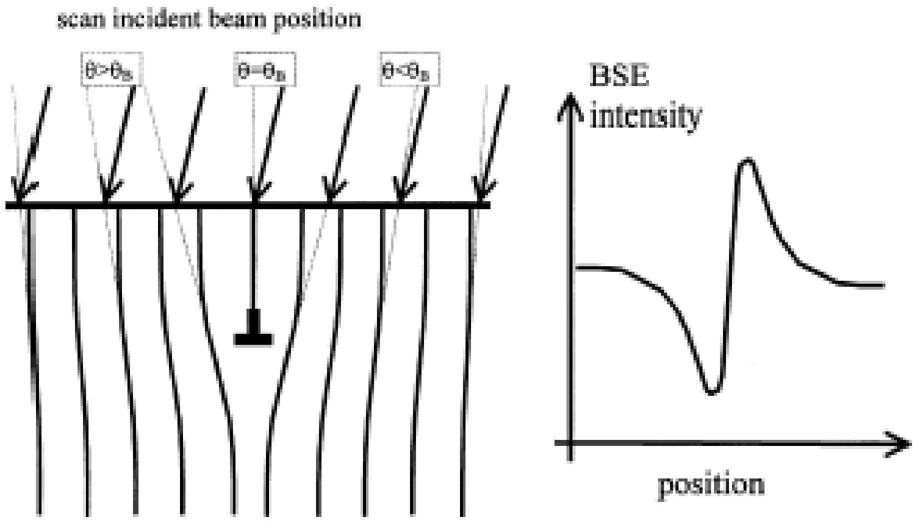

J. Ahmed *et al*, J. Microscopy **195**, 197 (1999).

ECCI of Screw Dislocation in 4H-SiC (0001)

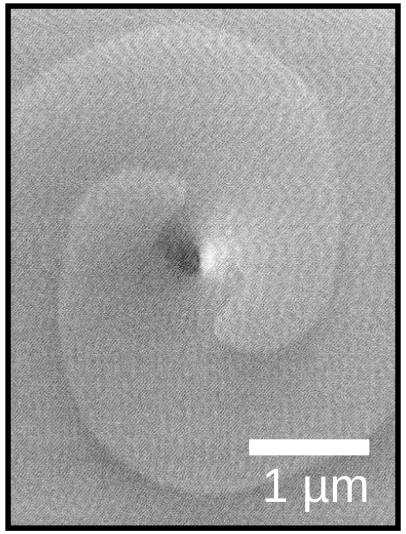

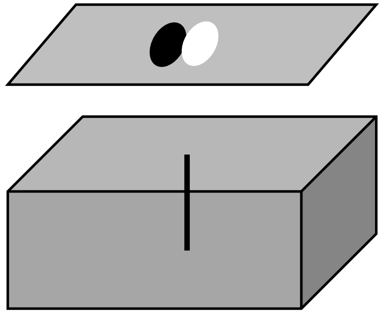

Dark-Light Spot Feature

Surface Penetrating Vertical Dislocation

Y.N. Picard *et al*, J. Appl. Phys. **104**, (2008) 124906.

ECCI of Edge Dislocation in $SrTiO_3$ (100)

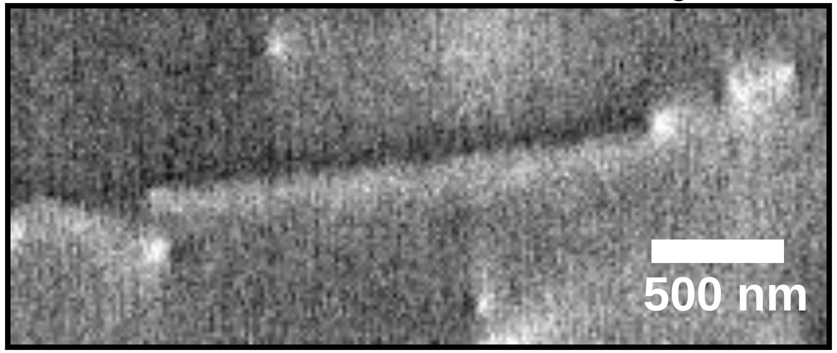

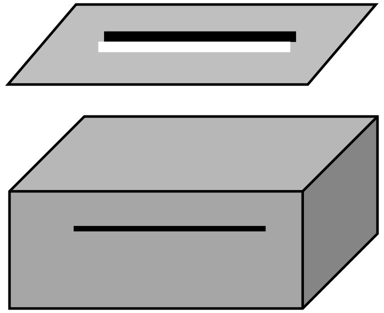

Dark-Light Line Feature

Sub-Surface Horizontal Dislocation

Dislocation Line Direction – Insights from Etching

$SrTiO_3$ (100): HF acid etching is defect selective

ECCI **SEM post-etching**

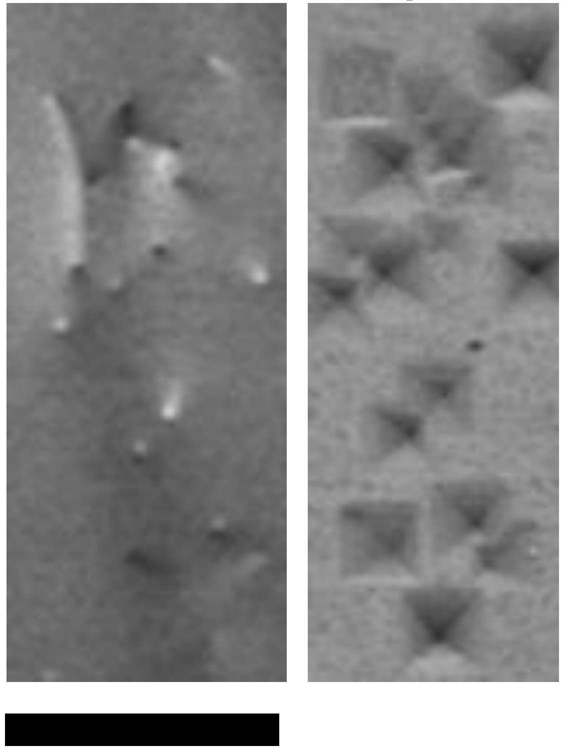

2 µm

Line feature is sub-surface, no etch feature

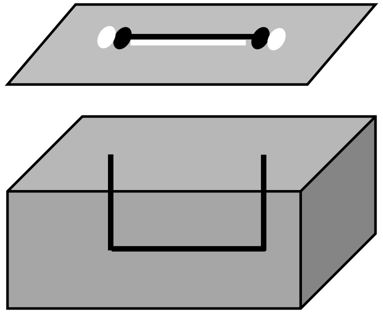

Half-loop configuration

ECCI **SEM post-etching**

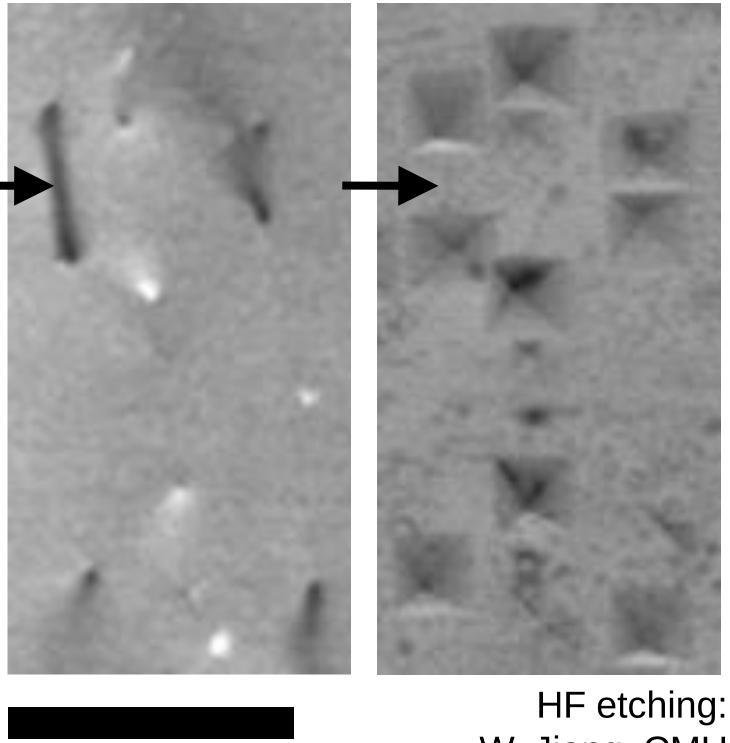

2 µm

HF etching:
W. Jiang, CMU

R.J. Kamaladasa and Y.N. Picard,, **Journal of Electronic Materials**, **40**(11), 2222-2227 (2011)

1:1 Correlation for surface penetrating dislocations

ECCI – Invisibility Criteria

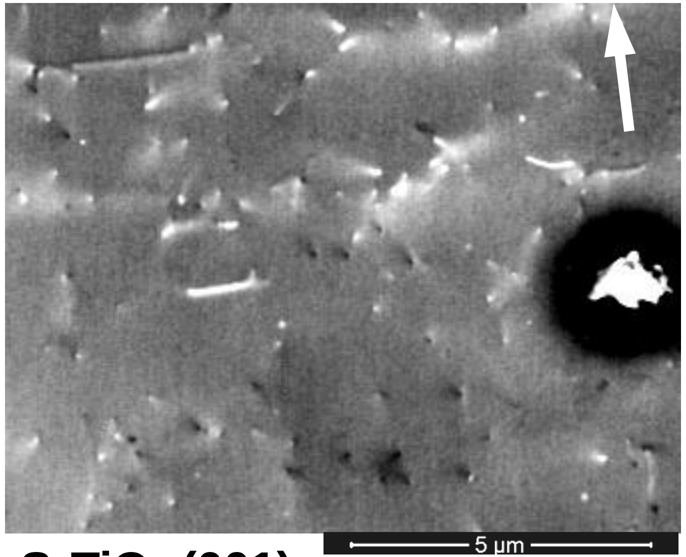

g = 100

SrTiO$_3$ (001)

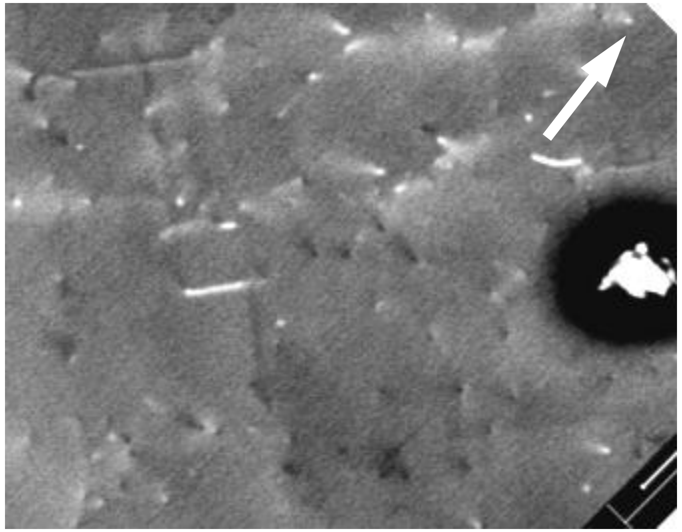

g = 110

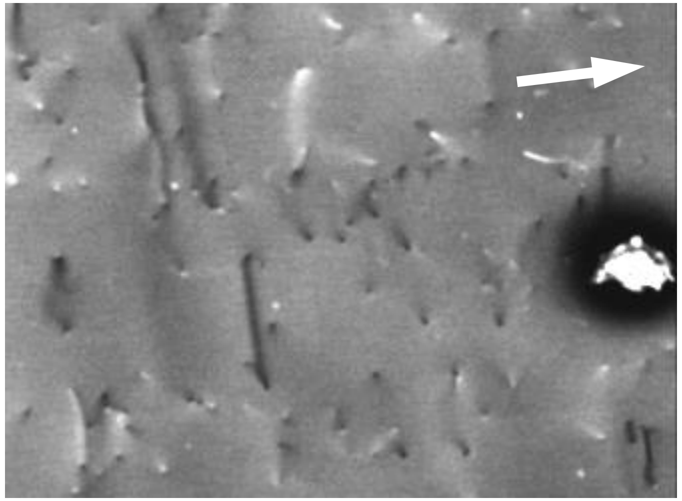

g = 010

g • b = 0 (screw)
g • b x u = 0 (edge)
Invisibility criteria

Dislocation line: u = <100>
Burgers vector: **b**
Diffraction vector: **g**

Independent variable
g vector

Dependent variable
Dislocation feature contrast (strong, weak, invisible)

Feature shape
u (dislocation line)

Result:
b identification (dislocation determination)

Yoosuf N. Picard, Materials Science & Engineering
Carnegie Mellon

ECCI – Various Dislocation Interactions

$SrTiO_3$ (001)

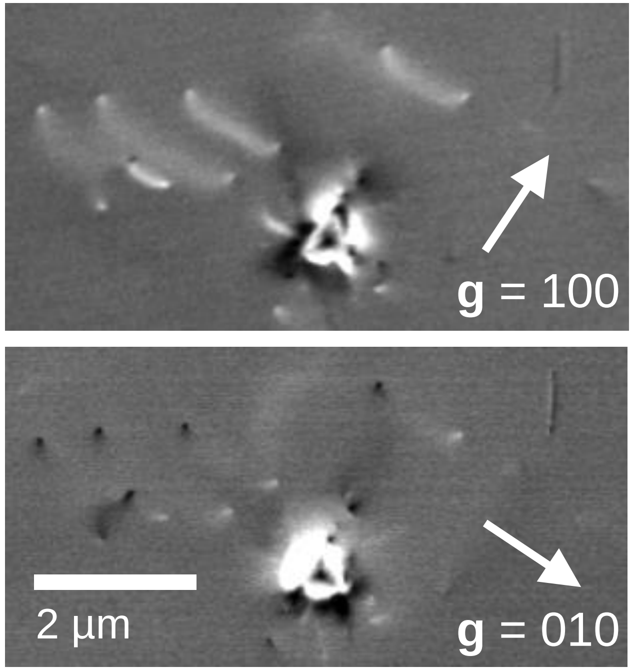

Surface-penetrating half-loops

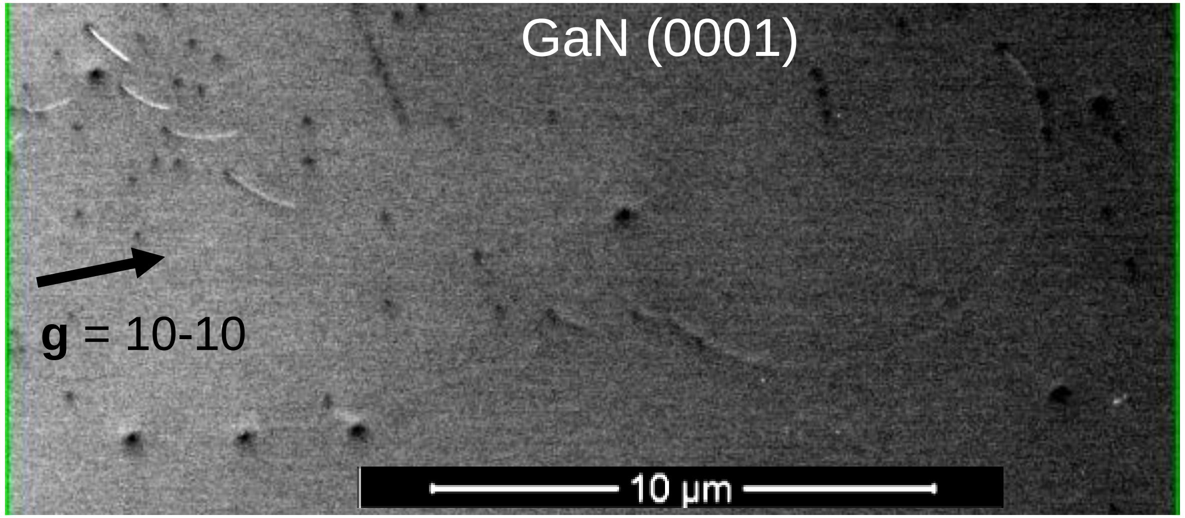

Y.N. Picard et. al. **Microscopy Today**. **20** (2), 12-16 (2012).

Sub-surface dislocation loops

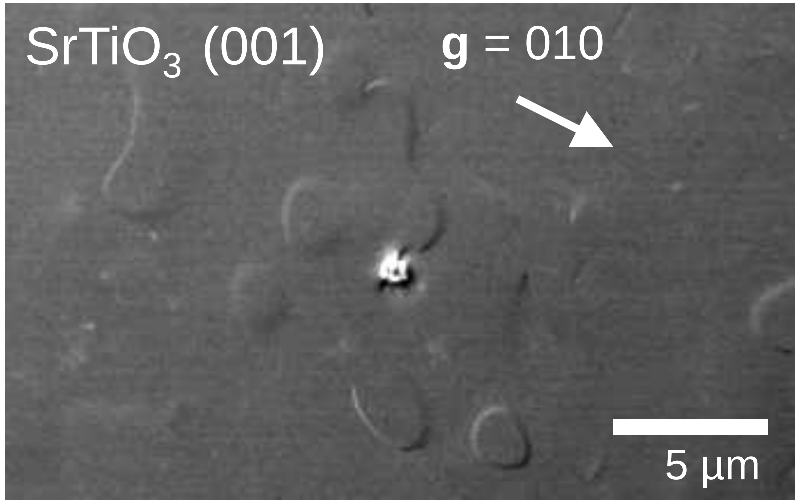

Y.N. Picard et. al. **Microscopy Today**. **20** (2), 12-16 (2012).

Dislocations along slip line

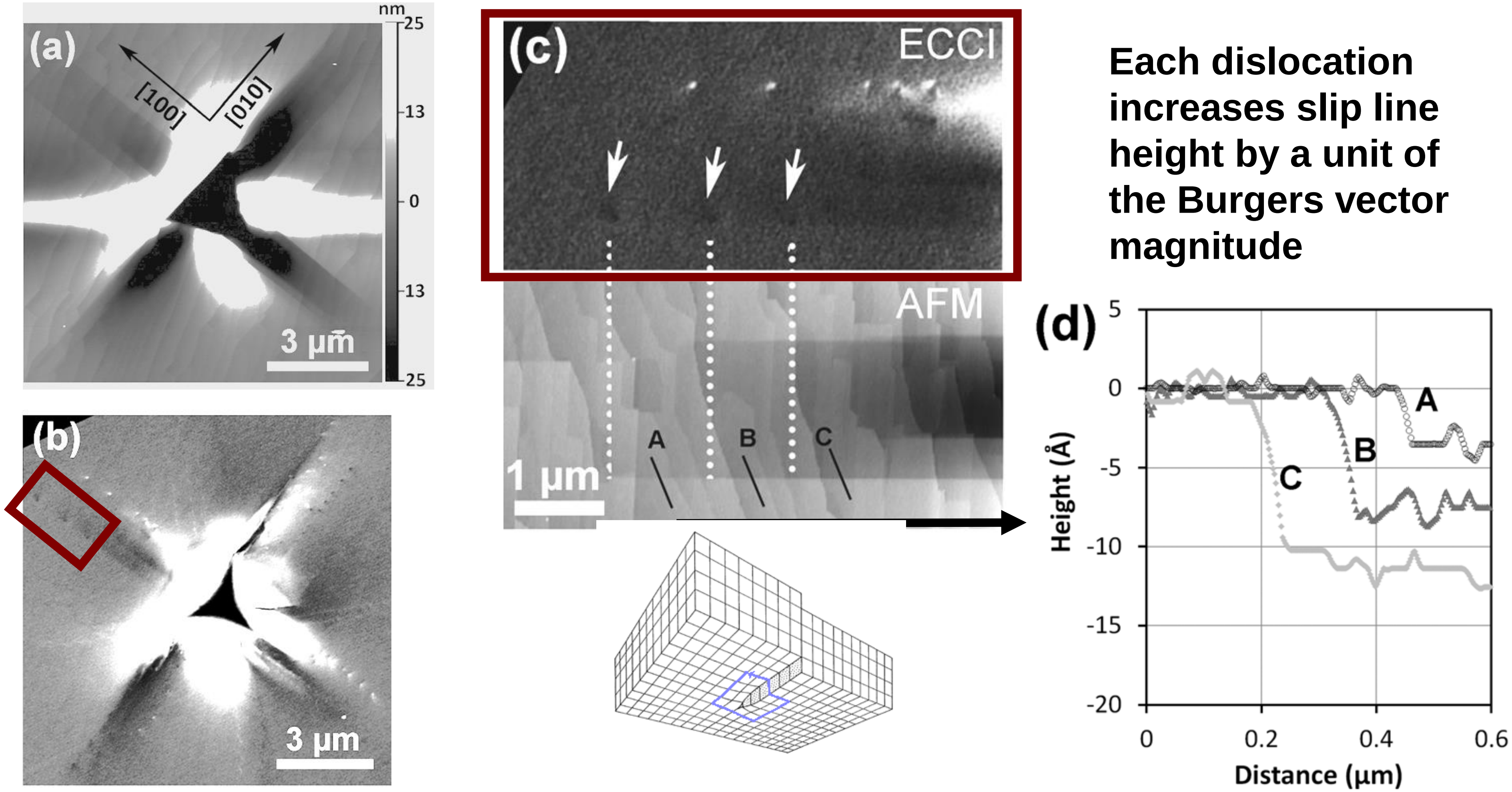

Each dislocation increases slip line height by a unit of the Burgers vector magnitude

W. Jiang, R.J. Kamaladasa, Y. Lu, R. Berechman, P.A. Salvador, J.A. Bain, Y.N. Picard, M. Skowronski, “Local heating-induced plastic deformation in resistive switching devices” **Journal of Applied Physics**, **110**(5), 054514 (2011).

Accurate Simulation of ECCI features

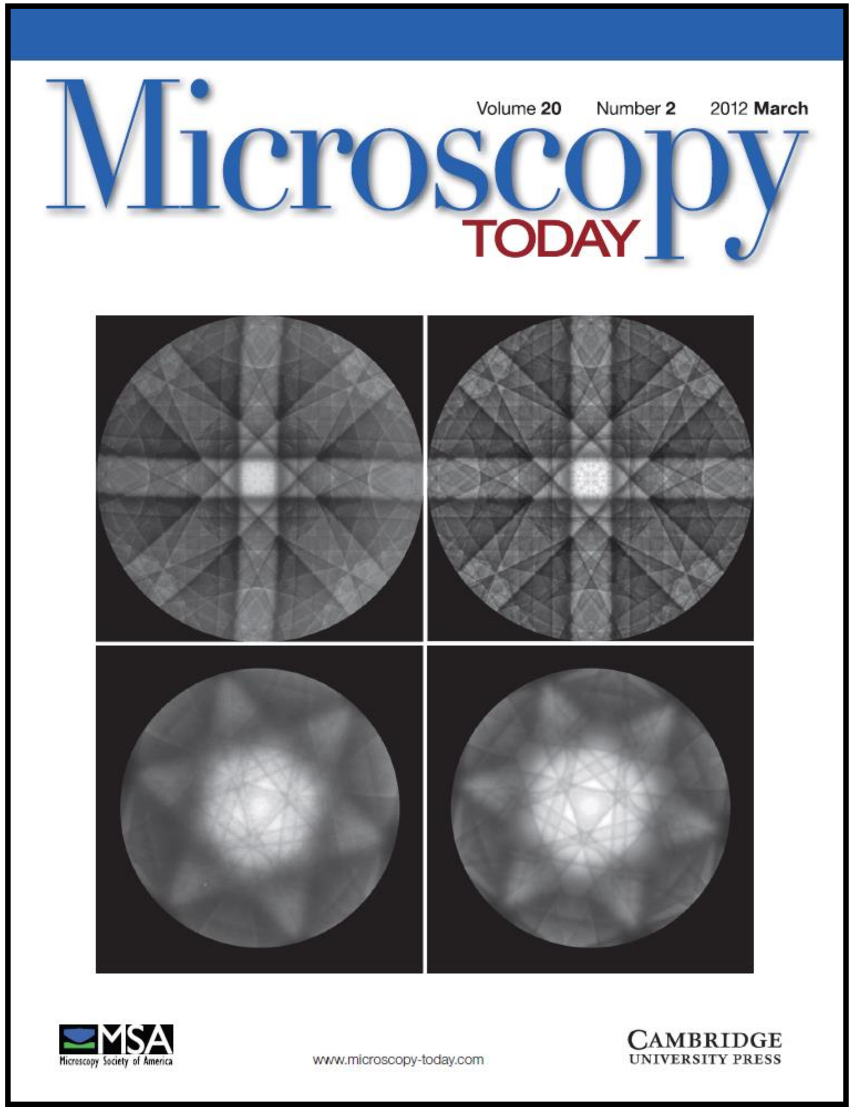

GaSb (001)

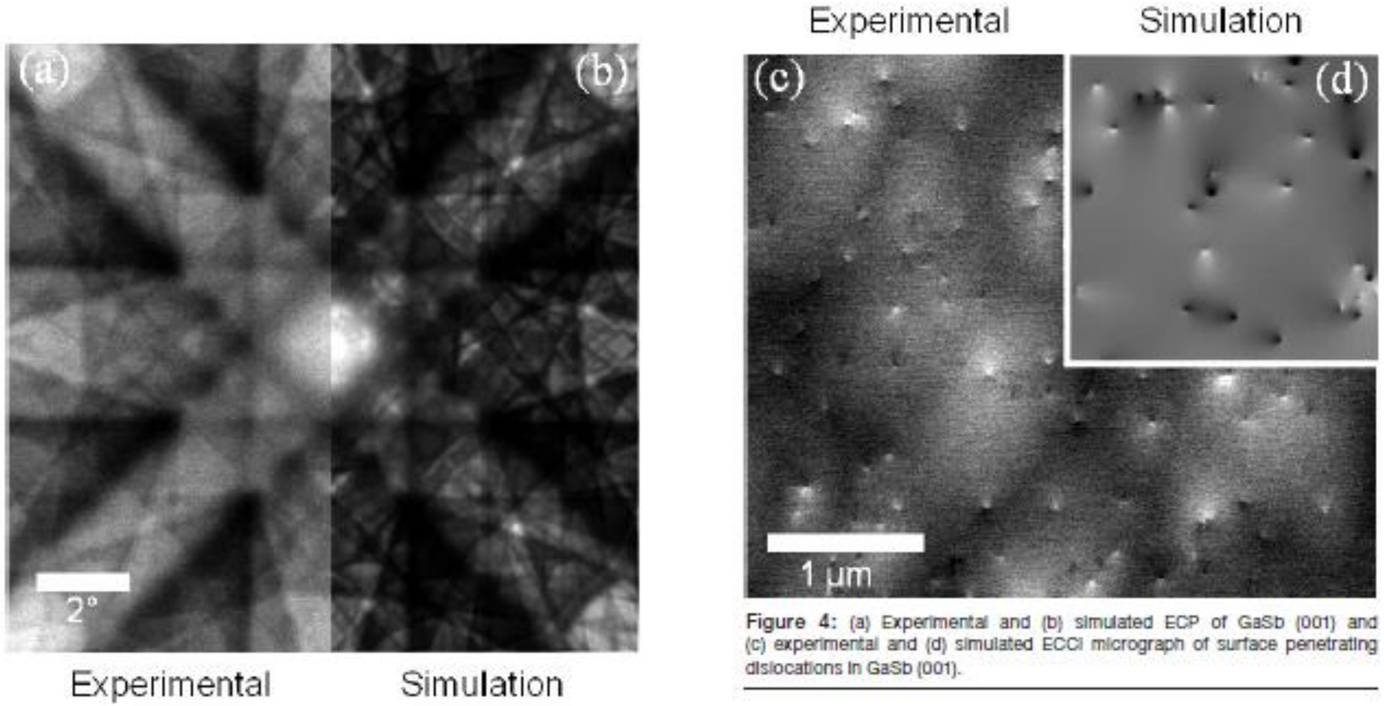

Figure 4: (a) Experimental and (b) simulated ECP of GaSb (001) and (c) experimental and (d) simulated ECCI micrograph of surface penetrating dislocations in GaSb (001).

Y.N. Picard, et. al., “Future prospects for defect and strain analysis in the SEM via electron channeling” **Microscopy Today**. **20** (2), 12-16 (2012).

Accurate Simulation of ECCI features

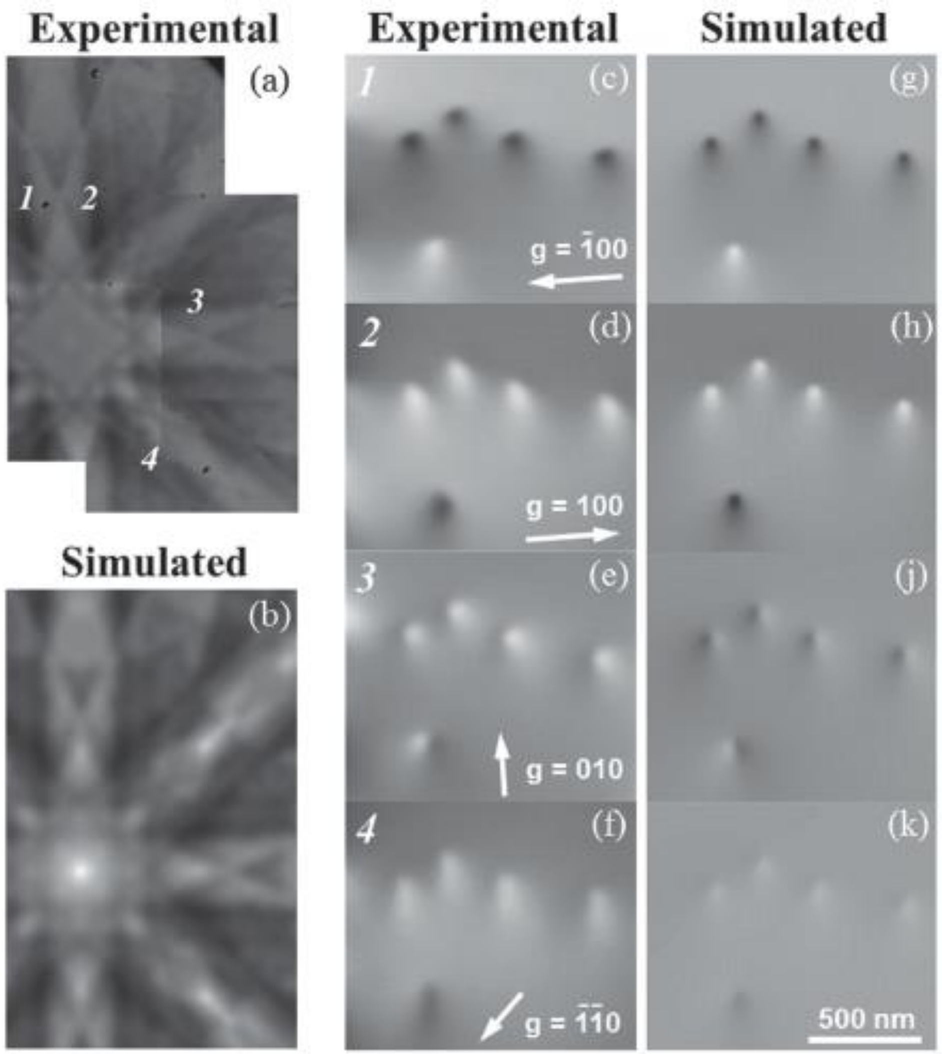

$SrTiO_3$ (001)
Perovskite single-crystal

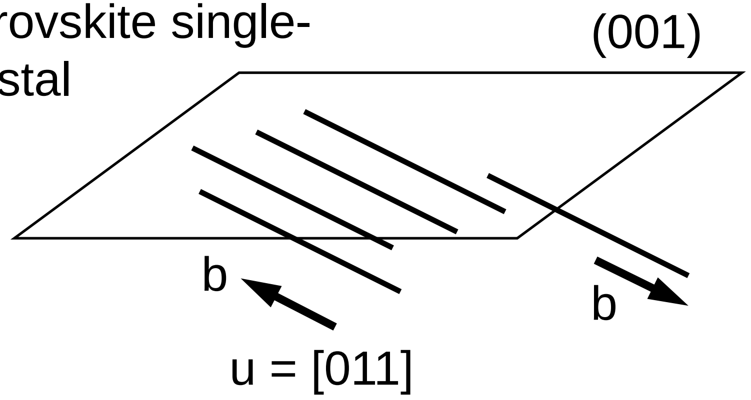

Screw dislocations inclined 45 degrees to (001) surface

Y.N. Picard, M. Liu, J. Lammatao, R.J. Kamaladasa, and M. De Graef, "Theory of Dynamical Electron Channeling Contrast Images of Near-Surface Crystal Defects" **Ultramicroscopy**, **146**, 71-78 (2014).

Non-destructive Mapping – Pre/Post Growth

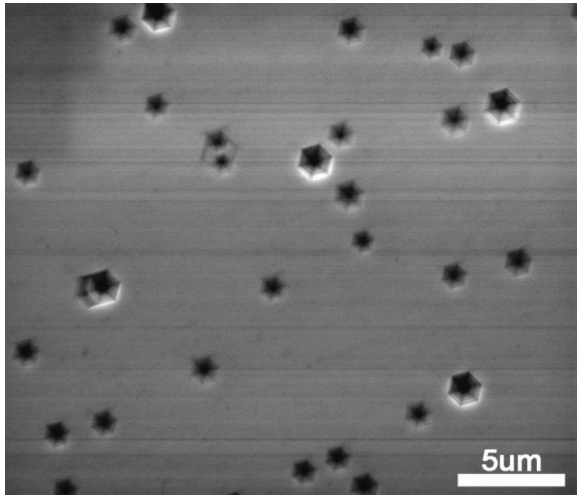

Wet etched surface of GaN homoepitaxy after growth

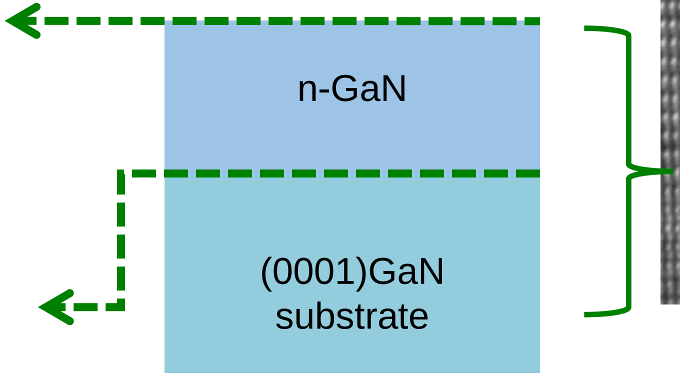

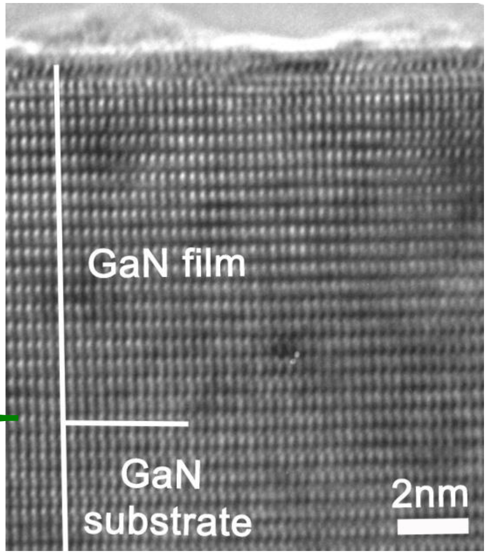

Cross sectional TEM images of 10nm GaN grown on (0001)GaN substrate

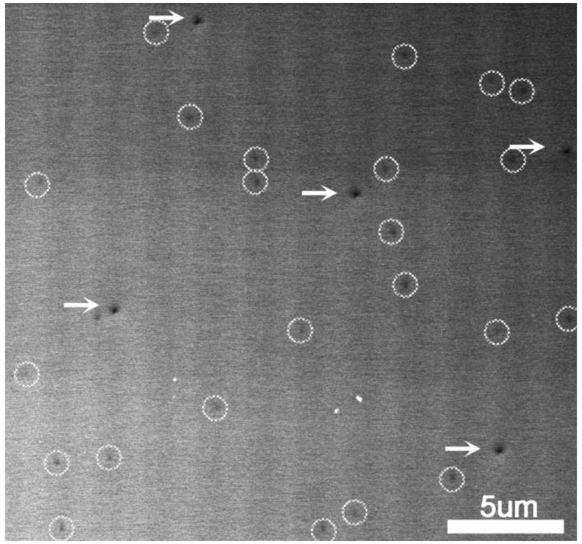

ECCI image of the (0001)GaN substrate before growth

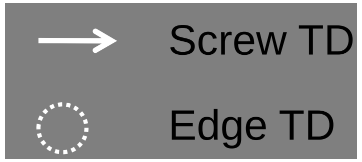

✓No new dislocations

✓All dislocations from the substrate propagate to homoepitaxial film

F. Liu, et. al., **Journal of Crystal Growth**, **387**, 16-22 (2014).

ECCI of $In_{0.1}Ga_{0.9}N$/GaN Multi-Quantum Wells

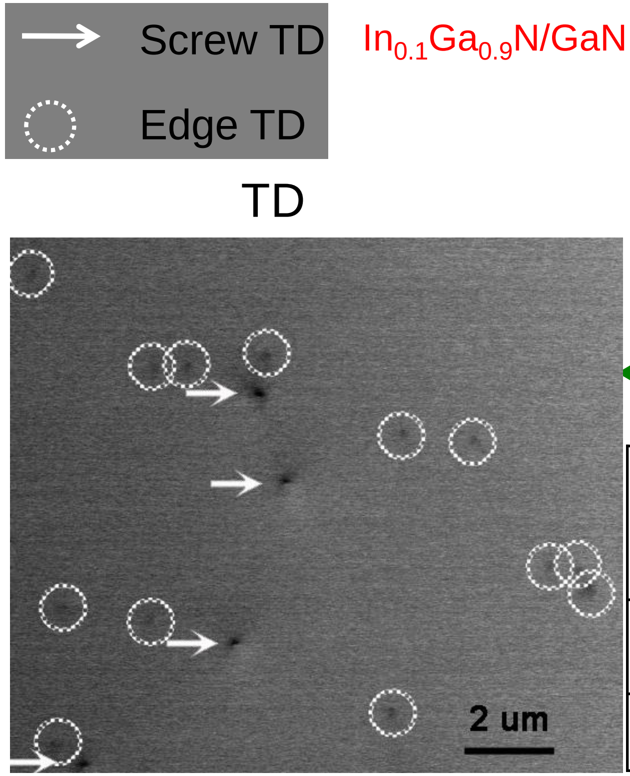

TD

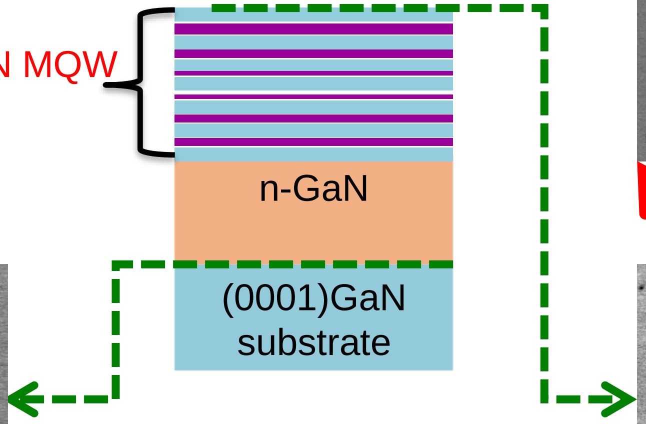

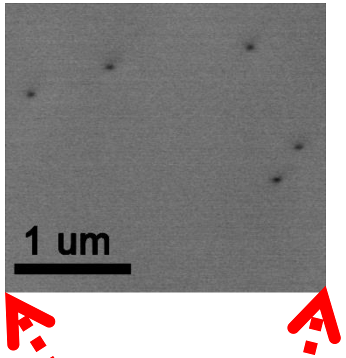

Topographic mode

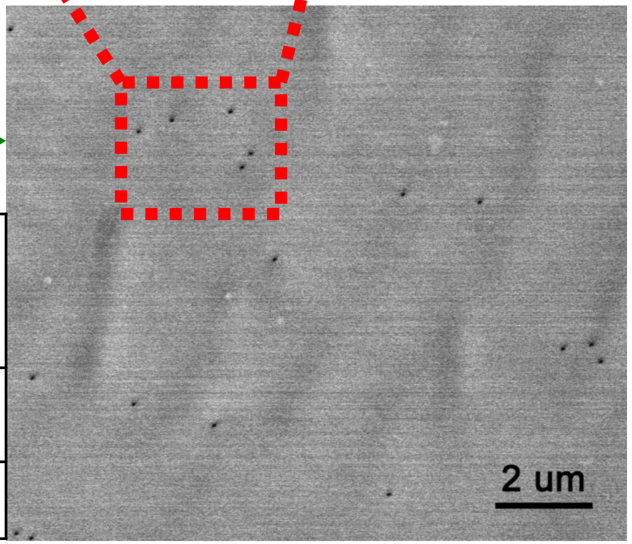

V-defects

Density ($10^6 cm^{-2}$)	Average	σ
V-defect	5.5	2.5
TD	5.5	2.5

ECCI image of (0001) GaN substrate before growth

One-to-One Correlation

SEM image of as grown surface of $In_{0.1}Ga_{0.9}N$/GaN MQW (non-channeling condition)

F. Liu, et. al., **Journal of Crystal Growth**, **387**, 16-22 (2014).

ECCI of GaP on Si (100)

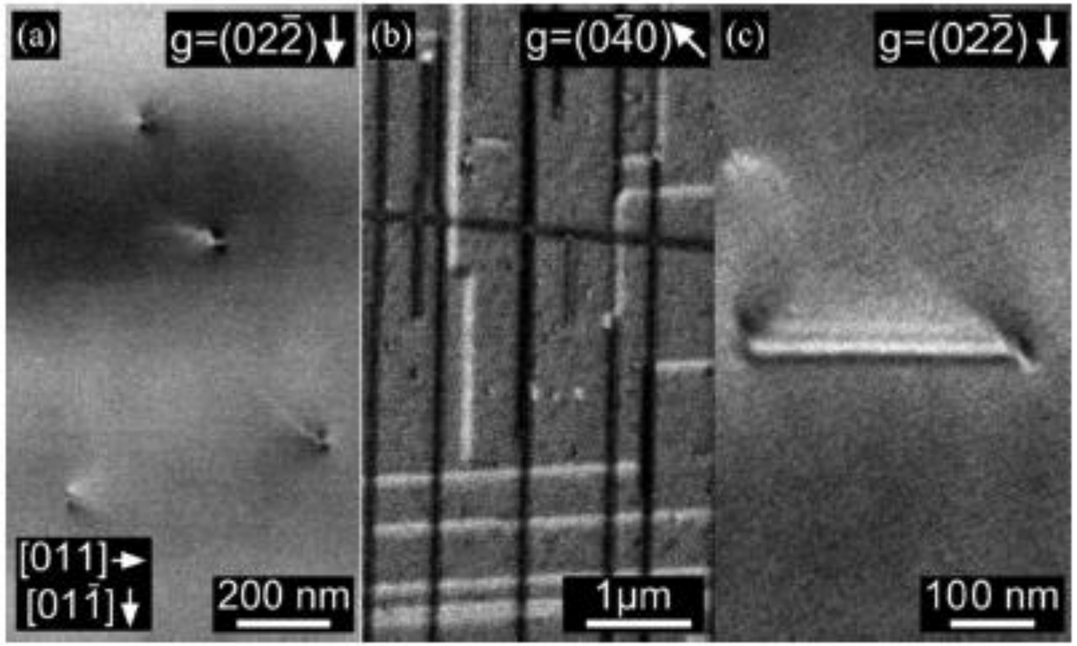

Threading Dislocations **Misfit Dislocations** **Stacking Fault**

S. D. Carnevale, J. I. Deitz, T. J. Grassman, J. A. Carlin, Y.N. Picard, M. De Graef, S. A. Ringel, "Rapid Misfit Dislocation Characterization in Heteroepitaxial III-V/Si Thin Films by Electron Channeling Contrast Imaging" **Applied Physics Letters**, **104**, 232111 (2014).

S.D. Carnevale, J. Deitz, J. Carlin, Y.N. Picard, D.W. McComb, M. De Graef, S. Ringel, T.J. Grasssman, "Applications of Electron Channeling Contrast Imaging for the Rapid Characterization of Extended Defects in III-V/Si Heterostructures" **IEEE Journal of Photovoltaics**, **5**(2) 676-682 (2015).

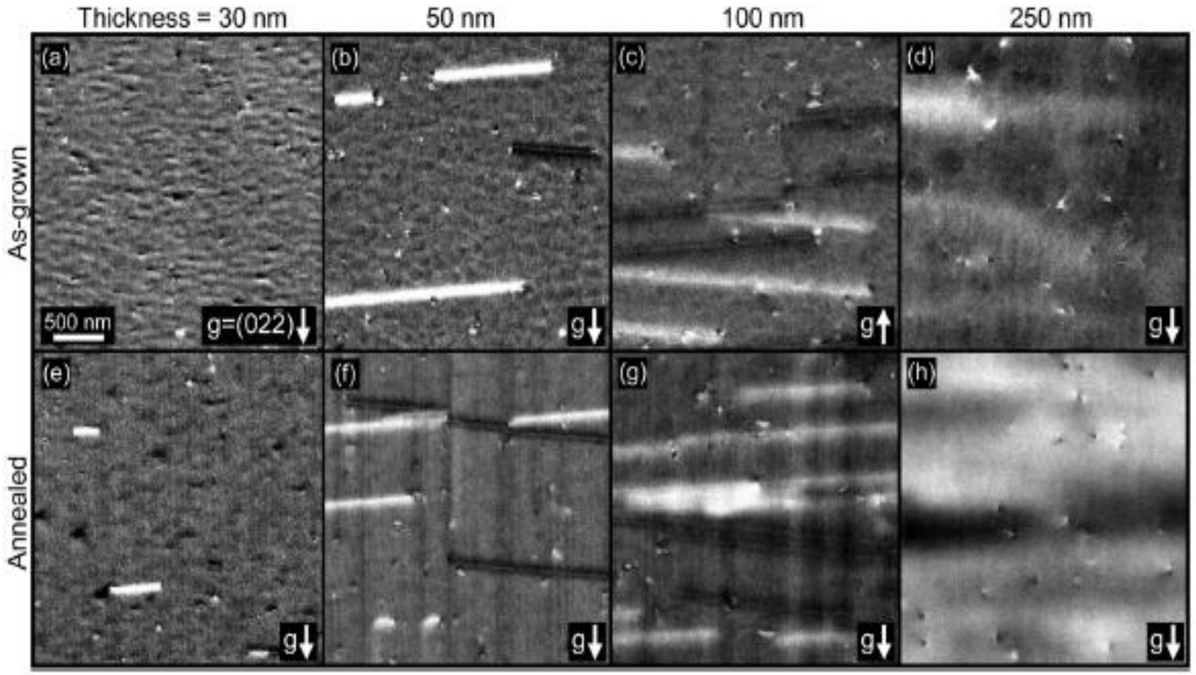

Anti-Phase Domain Boundaries

c-AFM of $La_{0.7}Sr_{0.3}MnO_3$

L. Balcells et. al., Phys. Rev. B. 92, 07[...]
(2015).

ECCI of $La_{0.7}Sr_{0.3}MnO_3$

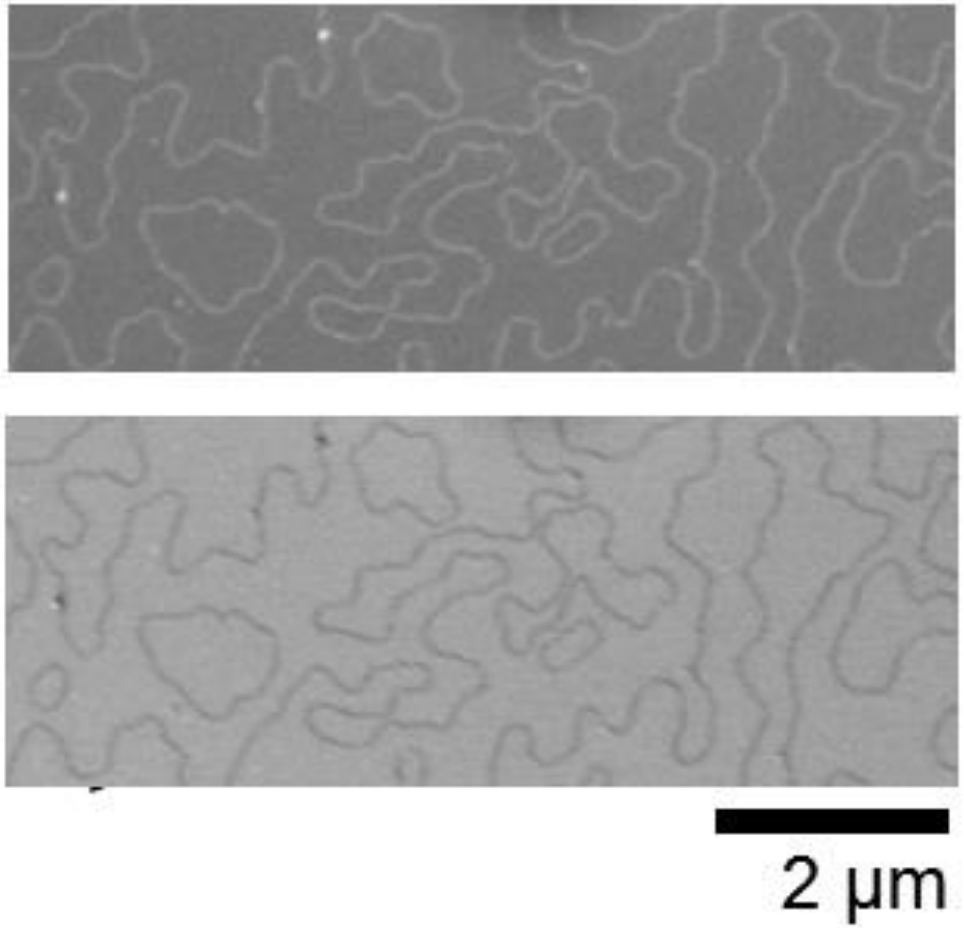

M. Yan et. al., Appl. Phys. Lett. 107, 041601 (2015).

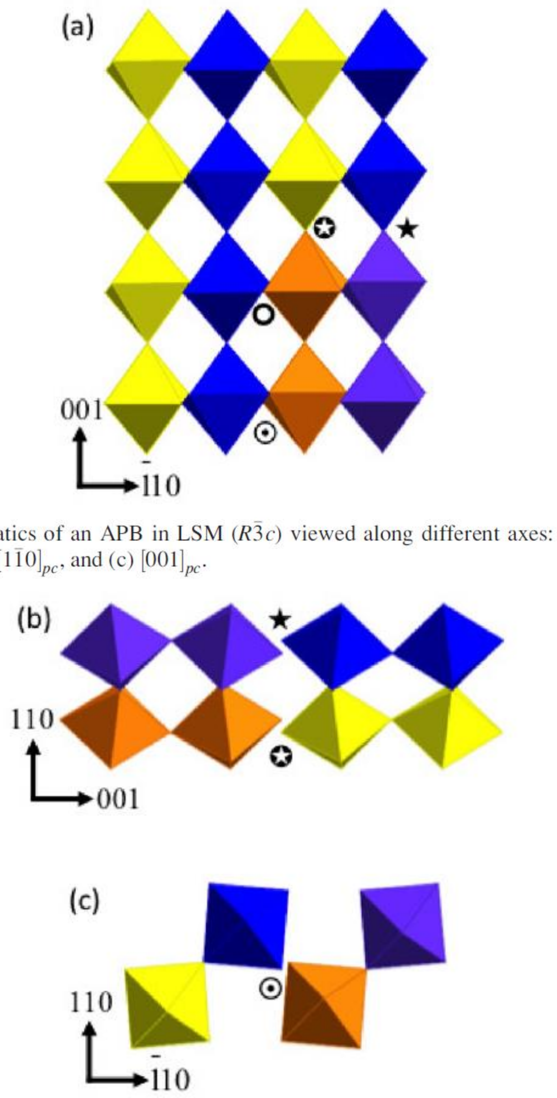

FIG. 6. Schematics of an APB in LSM ($R\bar{3}c$) viewed along different axes: (a) $[110]_{pc}$, (b) $[1\bar{1}0]_{pc}$, and (c) $[001]_{pc}$.

Si-Ge Misfit Dislocations

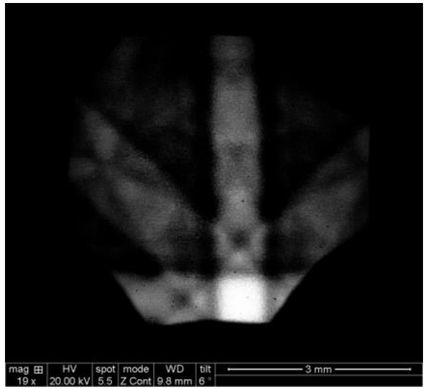

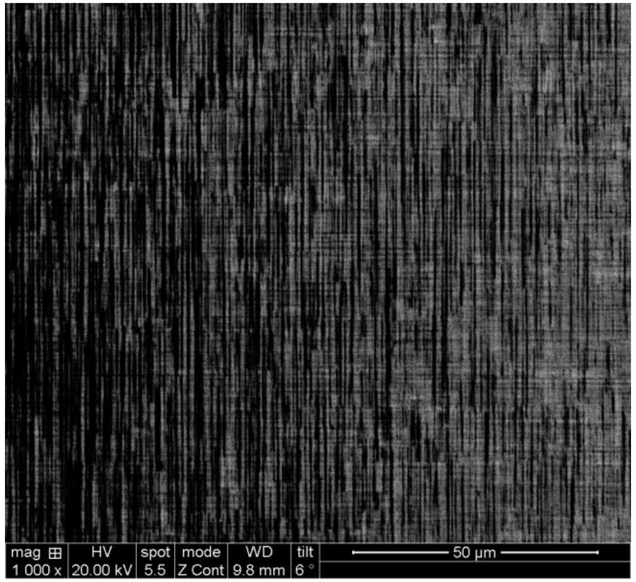

g = 2-20

SiGe (001) film on Si: High density of misfit dislocations on {110}

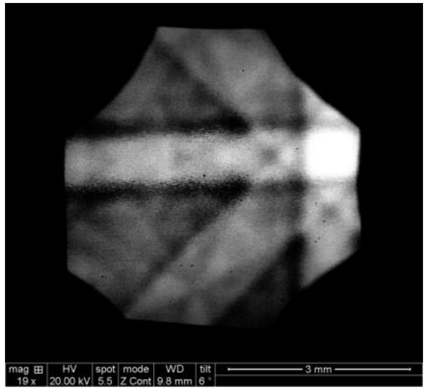

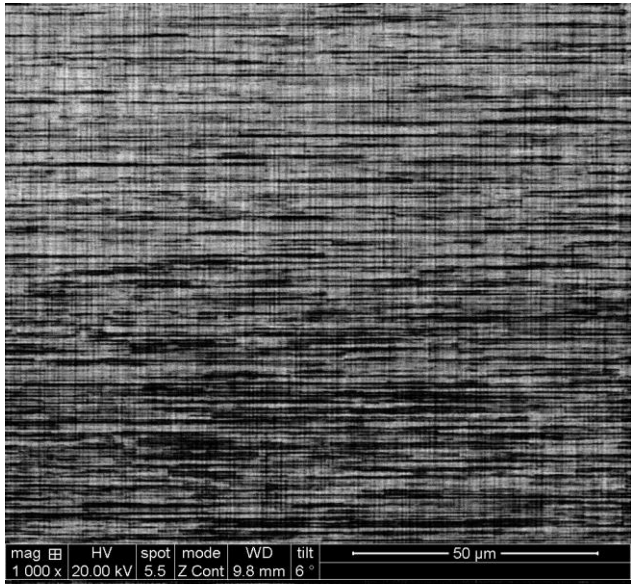

g = -2-20

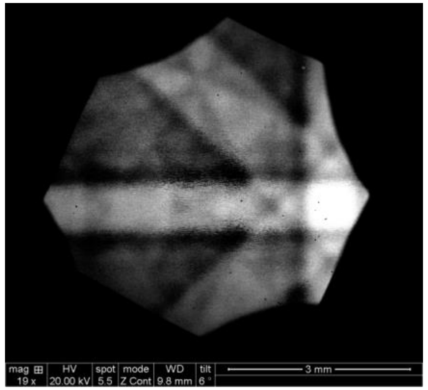

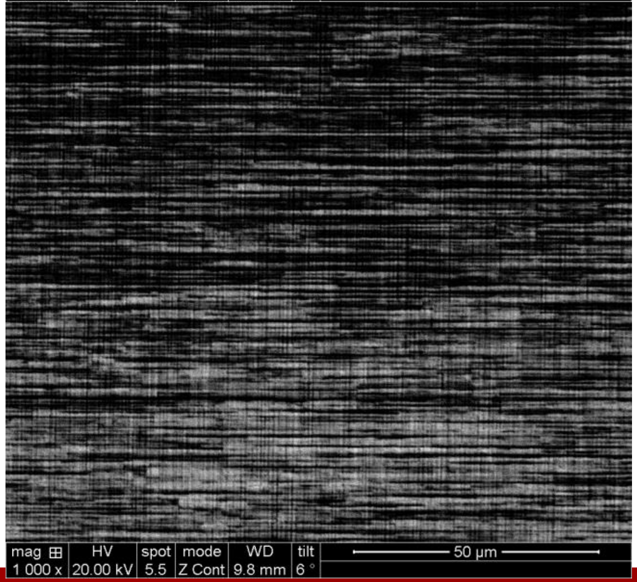

g = 220

Point Defect Clustering at Dislocations

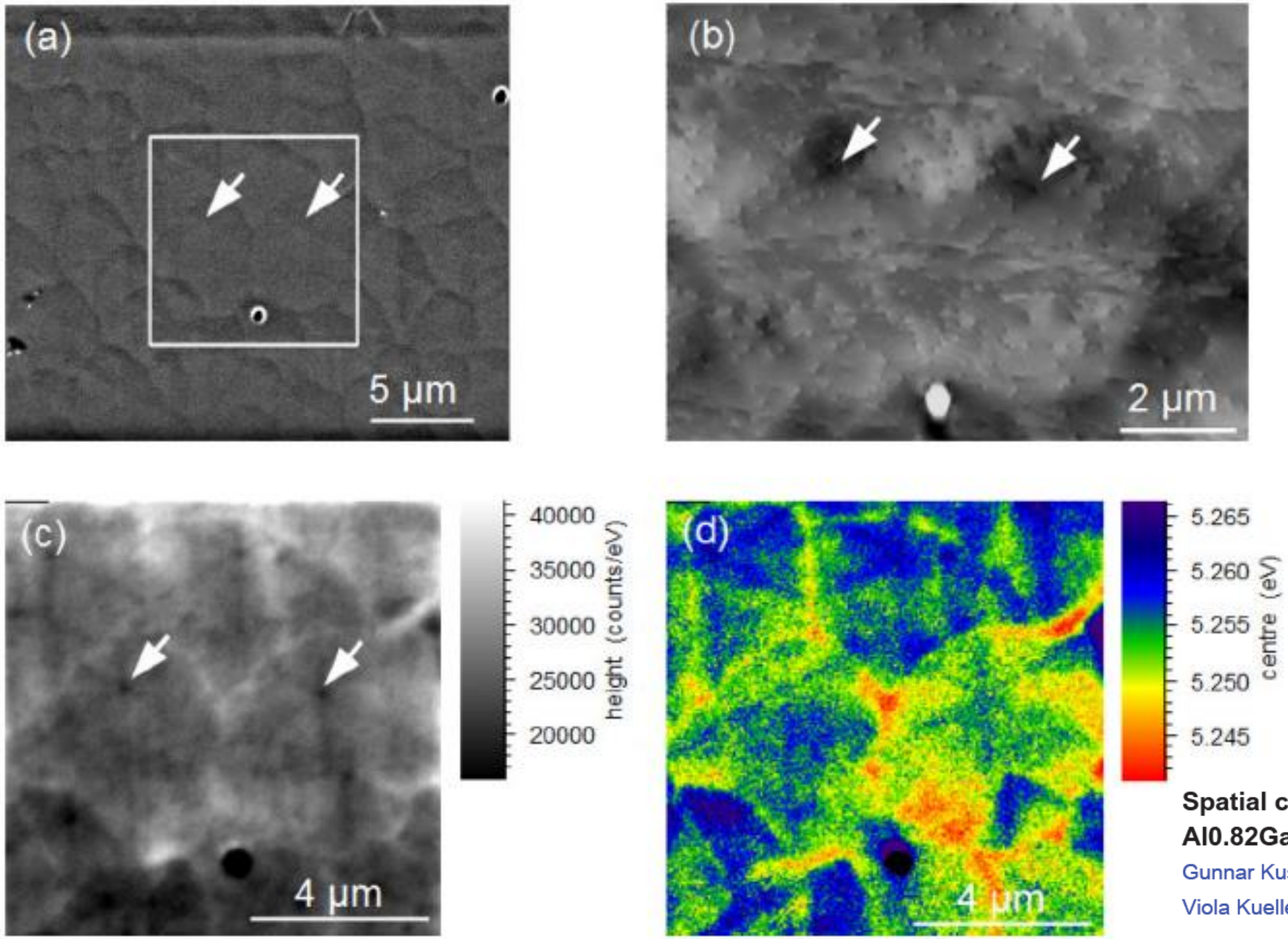

Screw dislocations from substrate nucleate hillocks

Hillock apex corresponds to drop in 5.32-5.39 eV NBE intensity

FIG. 3. SE (a) and ECCI image (b) as well as the intensity (c) and energy (d) of the CL NBE peak of sample B.

Spatial clustering of defect luminescence centers in Si-doped low resistivity Al0.82Ga0.18N

Gunnar Kusch, M. Nouf-Allehiani, Frank Mehnke, Christian Kuhn, Paul R. Edwards, Tim Wernicke, Arne Knauer, Viola Kueller, G. Naresh-Kumar, Markus Weyers, Michael Kneissl, Carol Trager-Cowan, and Robert W. Martin

Citation: Applied Physics Letters **107**, 072103 (2015); doi: 10.1063/1.4928667

ECCI correlation to Optoelectronic Behavior

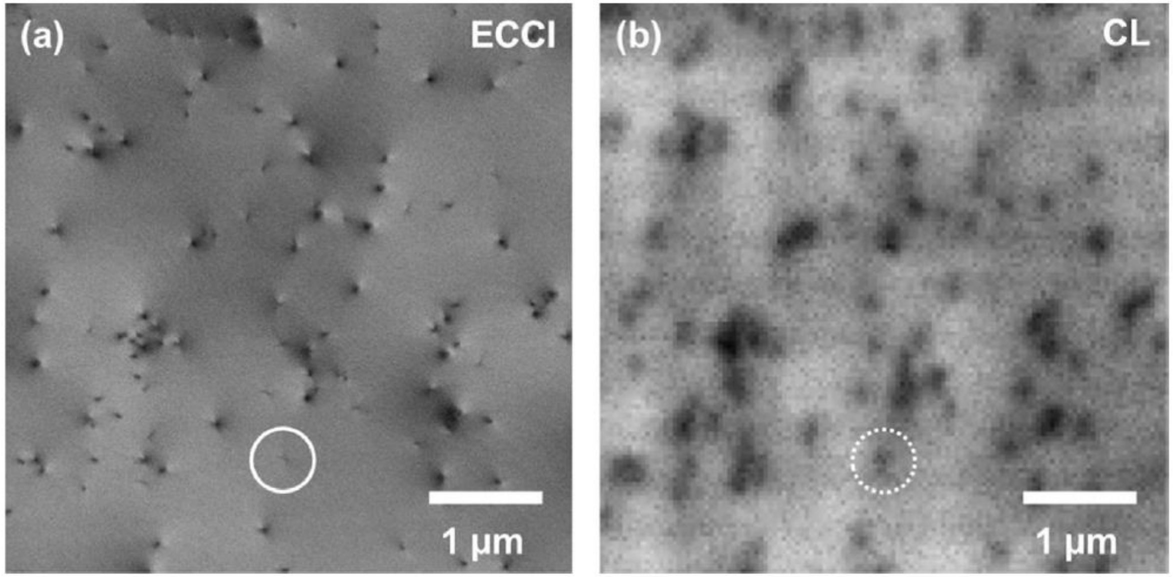

Materials Science in Semiconductor Processing 47 (2016) 44–50

Contents lists available at ScienceDirect

Materials Science in Semiconductor Processing

journal homepage: www.elsevier.com/locate/mssp

Electron channelling contrast imaging for III-nitride thin film structures

G. Naresh-Kumar*, D. Thomson, M. Nouf-Allehiani, J. Bruckbauer, P.R. Edwards, B. Hourahine, R.W. Martin, C. Trager-Cowan

Department of Physics, SUPA, University of Strathclyde, Glasgow G4 0NG, UK

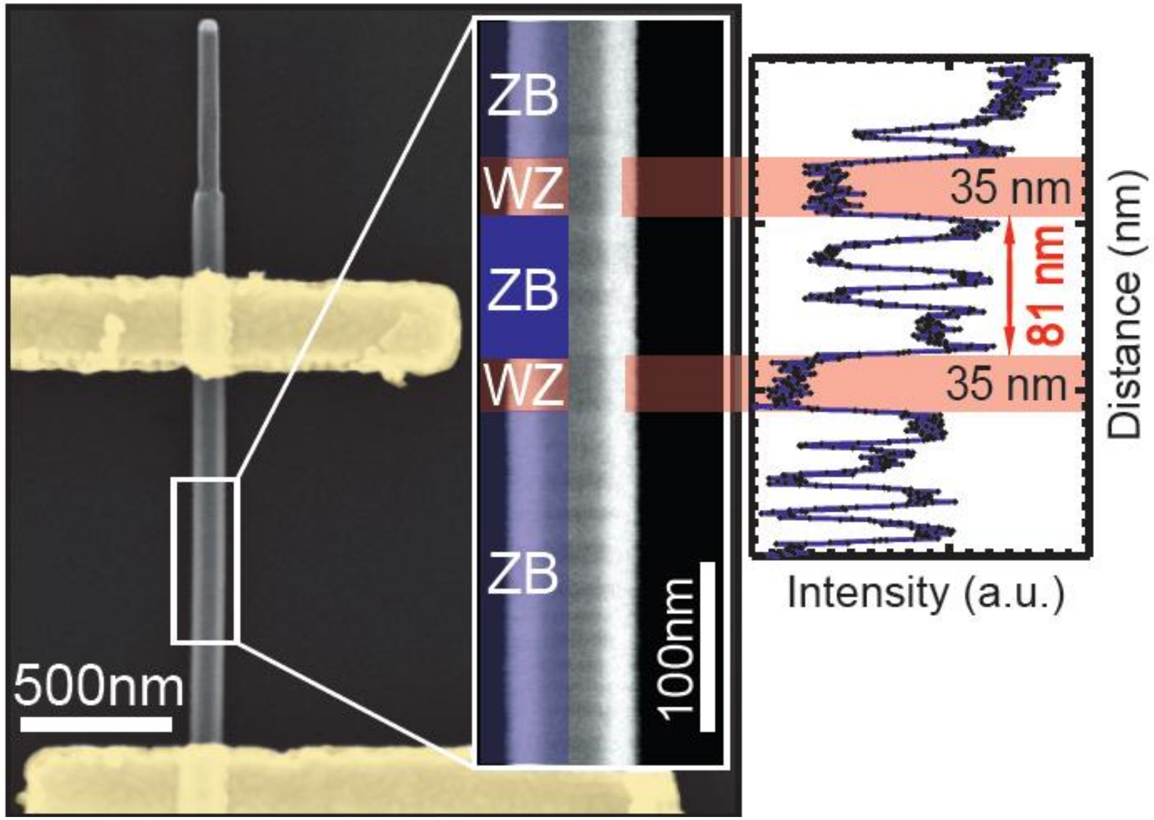

Single-electron transport in InAs nanowire quantum dots formed by crystal phase engineering

Malin Nilsson[1], Luna Namazi[1], Sebastian Lehmann[1], Martin Leijnse[1], Kimberly A. Dick[1,2], and Claes Thelander[1]
[1]Division of Solid State Physics and NanoLund, Lund University, Box 118,S-221 00 Lund, Sweden and
[2]Center for Analysis and Synthesis, Lund University, Box 124, S-221 00 Lund, Sweden

ECCI of Slip Bands in Steel

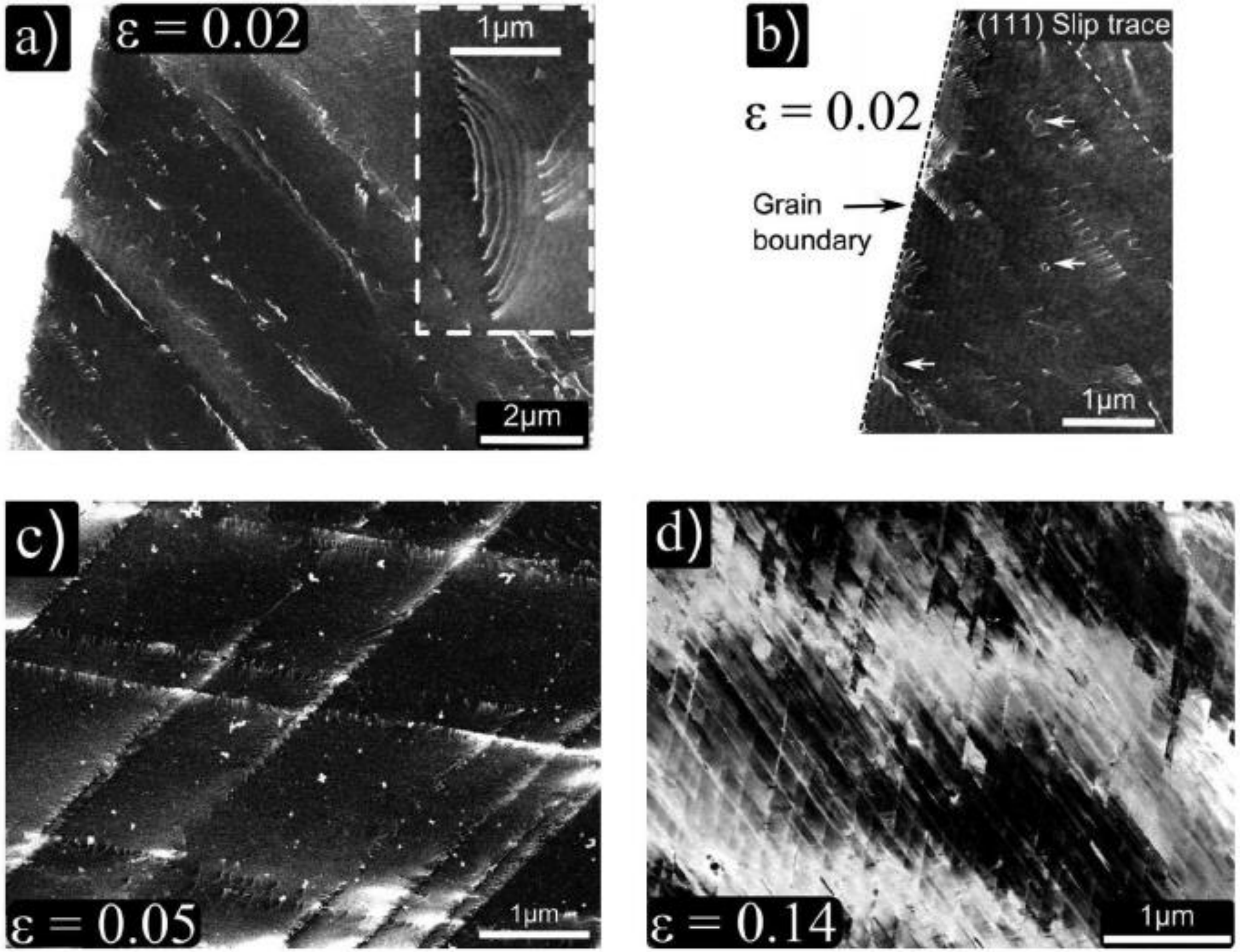

30 wt% Mn Steel under high strain rate → hardening behavior

Tensile axis is out-of-plane

a,b) planar dislocation glide {111} to slip band formation; c) slip bands have high stress between them


Acta Materialia 116 (2016) 188–199

Contents lists available at ScienceDirect

Acta Materialia

journal homepage: www.elsevier.com/locate/actamat

ELSEVIER

Full length article

Strain hardening by dynamic slip band refinement in a high-Mn lightweight steel

CrossMark

E. Welsch [a], D. Ponge [a, *], S.M. Hafez Haghighat [a], S. Sandlöbes [a, b], P. Choi [a, c], M. Herbig [a], S. Zaefferer [a], D. Raabe [a]

ECCI of Slip Bands and Dislocations Evolution in Steel

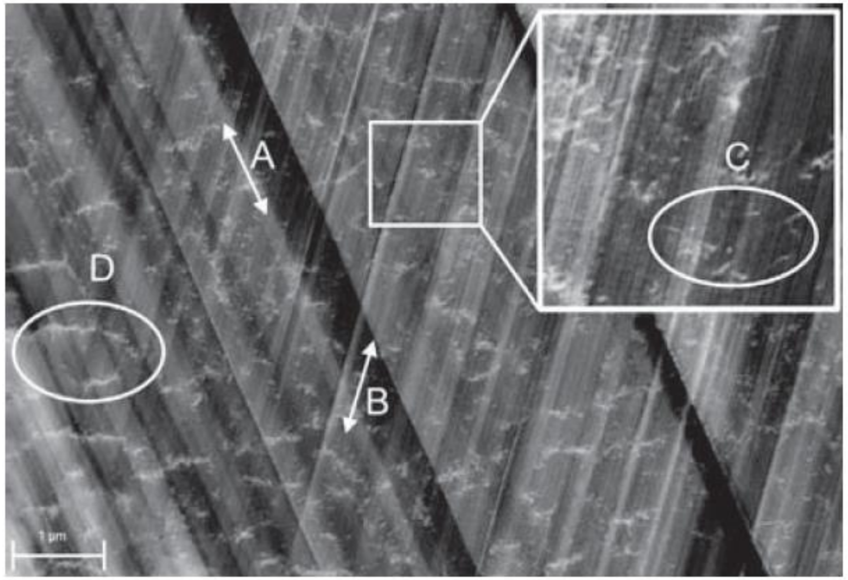

Fig. 4. Observation of features by ECCI: surface traces of different active slip planes (A, B), individual dislocations (C) (enlarged region) and dislocation structures such as veins (D).

ELSEVIER
CrossMark
Available online at www.sciencedirect.com
ScienceDirect
Acta Materialia 87 (2015) 86–99
Acta MATERIALIA
www.elsevier.com/locate/actamat

Effects of strain amplitude, cycle number and orientation on low cycle fatigue microstructures in austenitic stainless steel studied by electron channelling contrast imaging

J. Nellessen, S. Sandlöbes* and D. Raabe

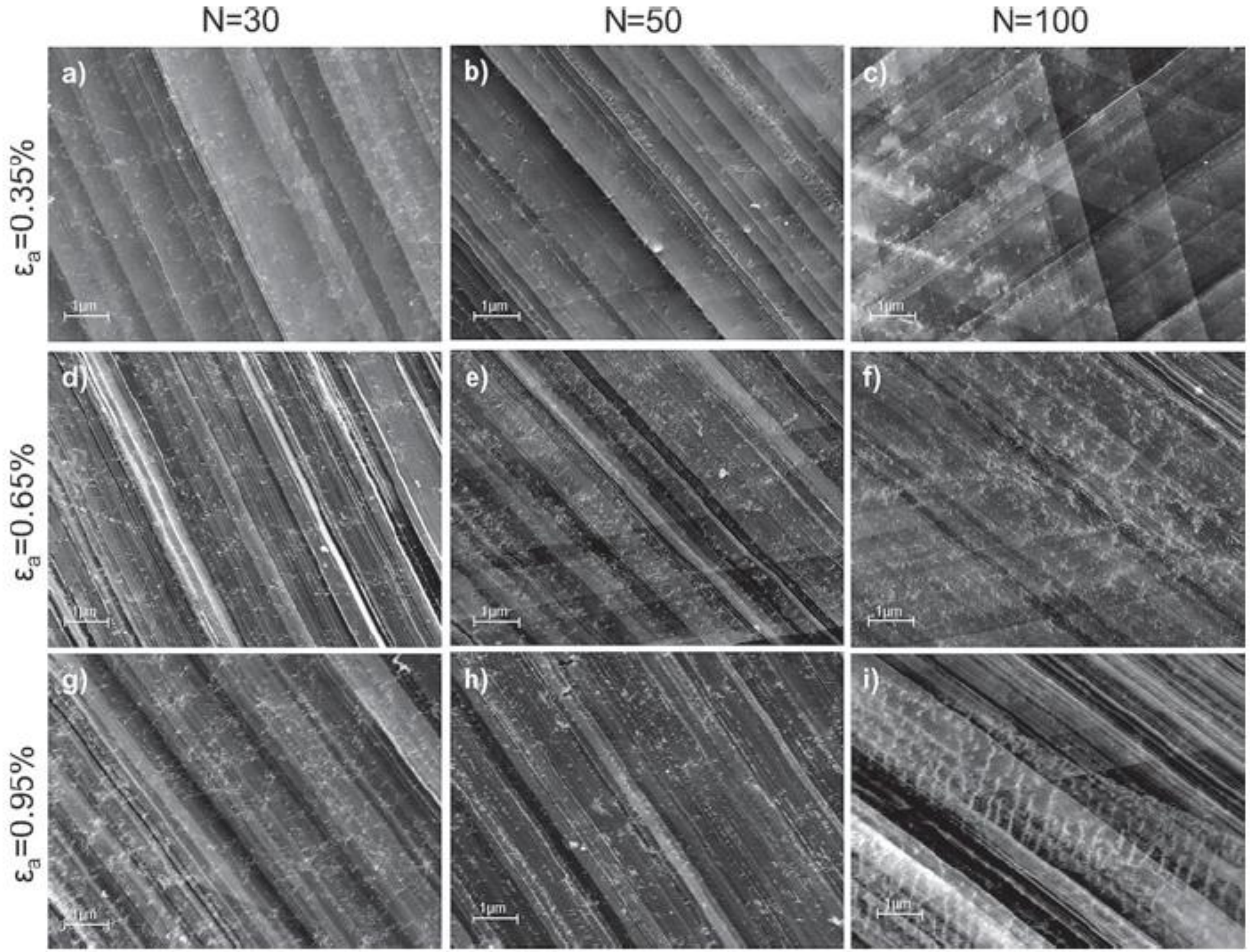

Sub-grain boundary characterization

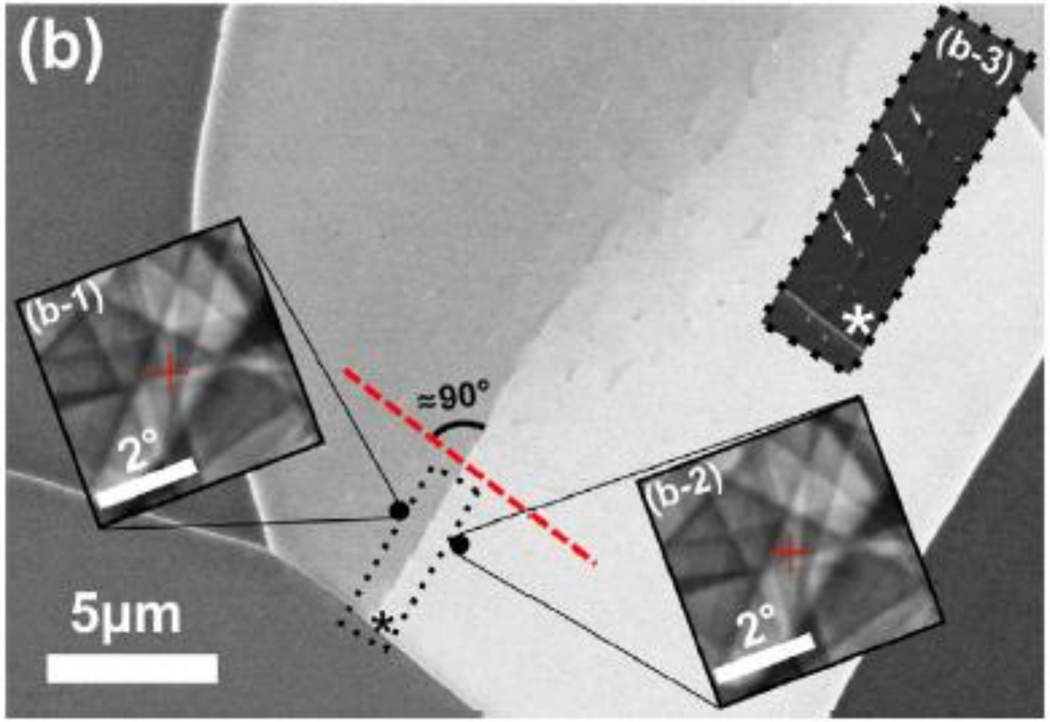

Fig. 1. (a) HR-SACP superimposed on a dynamical Kikuchi pattern simulated with the "Esprit DynamicS" software from Bruker. The red crosses in the HR-SACPs indicate the microscope optic axis. (b) ECC image of a sub-grain boundary showing HR-SACPs acquired from each side of the boundary reveals the direction of pattern shift (dotted red line) and the misorientation angle (≈0.13°). (For interpretation of the references to color in this figure legend, the reader is referred to the web version of this article.)

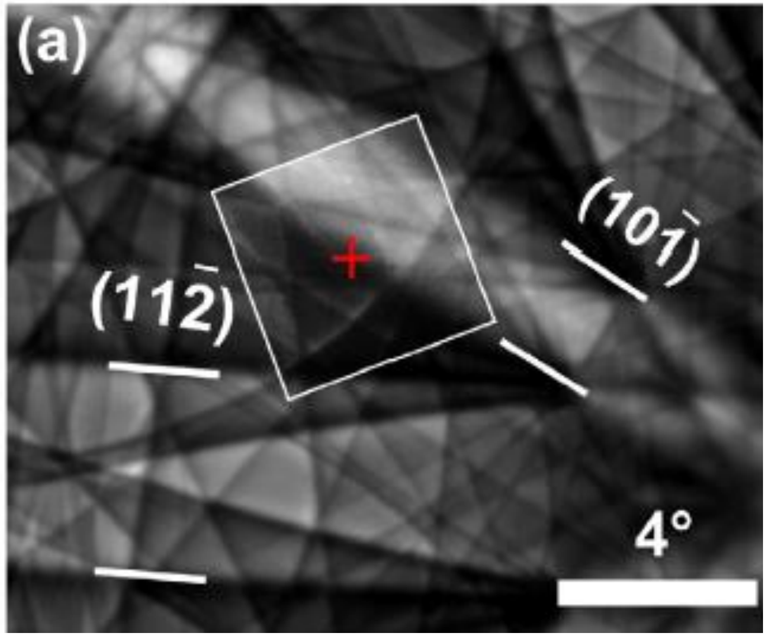

Scripta Materialia 109 (2015) 76–79

Contents lists available at ScienceDirect

Scripta Materialia

journal homepage: www.elsevier.com/locate/scriptamat

ELSEVIER

Accurate electron channeling contrast analysis of a low angle sub-grain boundary

CrossMark

H. Mansour [a,*], M.A. Crimp [b], N. Gey [a,c], N. Maloufi [a,c,*]

Inverted ECCI – High Resolution Bright-Field

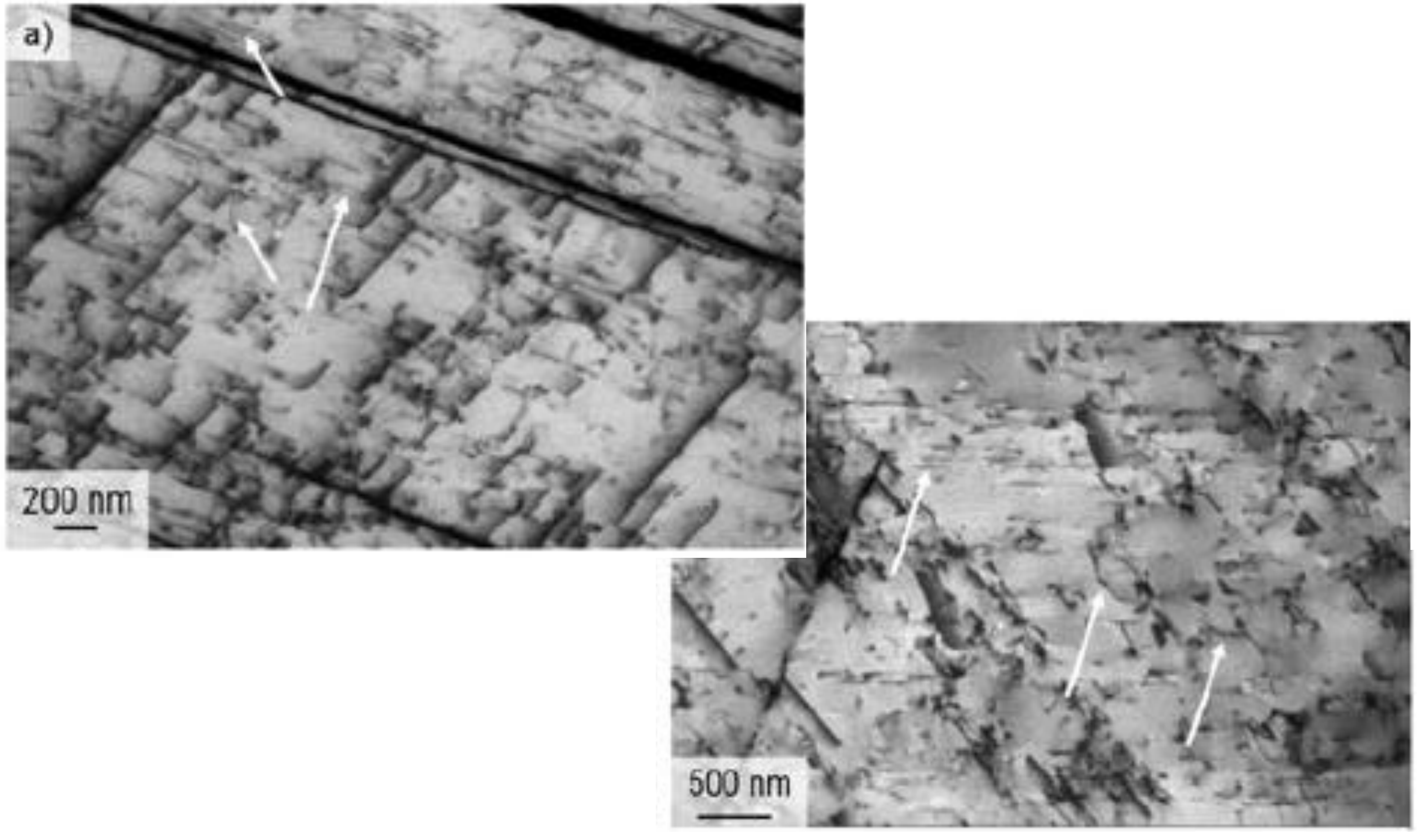

Figure 6. Inverted ECCI micrographs of a high-alloy TRIP steel (G-X5CrMnNi16.6.6) after tensile deformation at room temperature up to 8% of elongation. (a) Mixture of deformation bands, individual SFs and regular dislocations. (b) Development of a new deformation band by grouping of several individual SFs along the same slip plane and regular dislocations in the austenitic matrix.

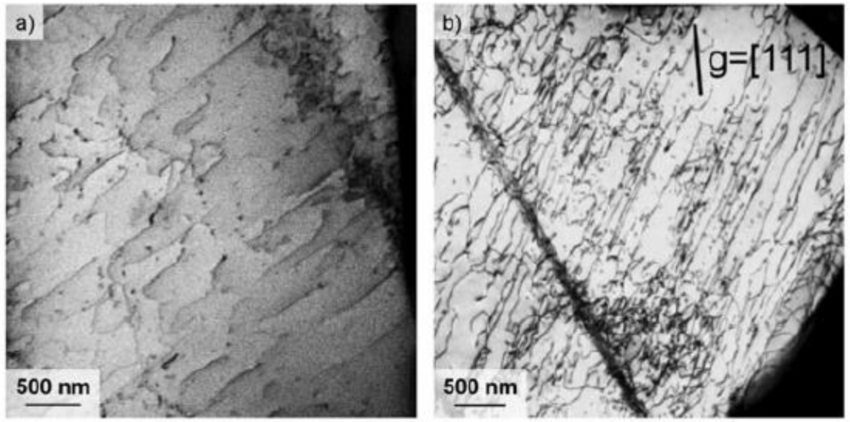

Figure 8. Comparison between inverted ECCI (a) and convential TEM (b) micrograph of the dislcation arrangement in a globular γ-TiAl grain. [after 65]. Details see Figure 7.

Philosophical Magazine

Taylor & Francis

ISSN: 1478-6435 (Print) 1478-6443 (Online) Journal homepage: http://www.tandfonline.com/loi/tphm20

Case studies on the application of high-resolution electron channelling contrast imaging – investigation of defects and defect arrangements in metallic materials

Anja Weidner & Horst Biermann

ECCI of a High Entropy Alloy

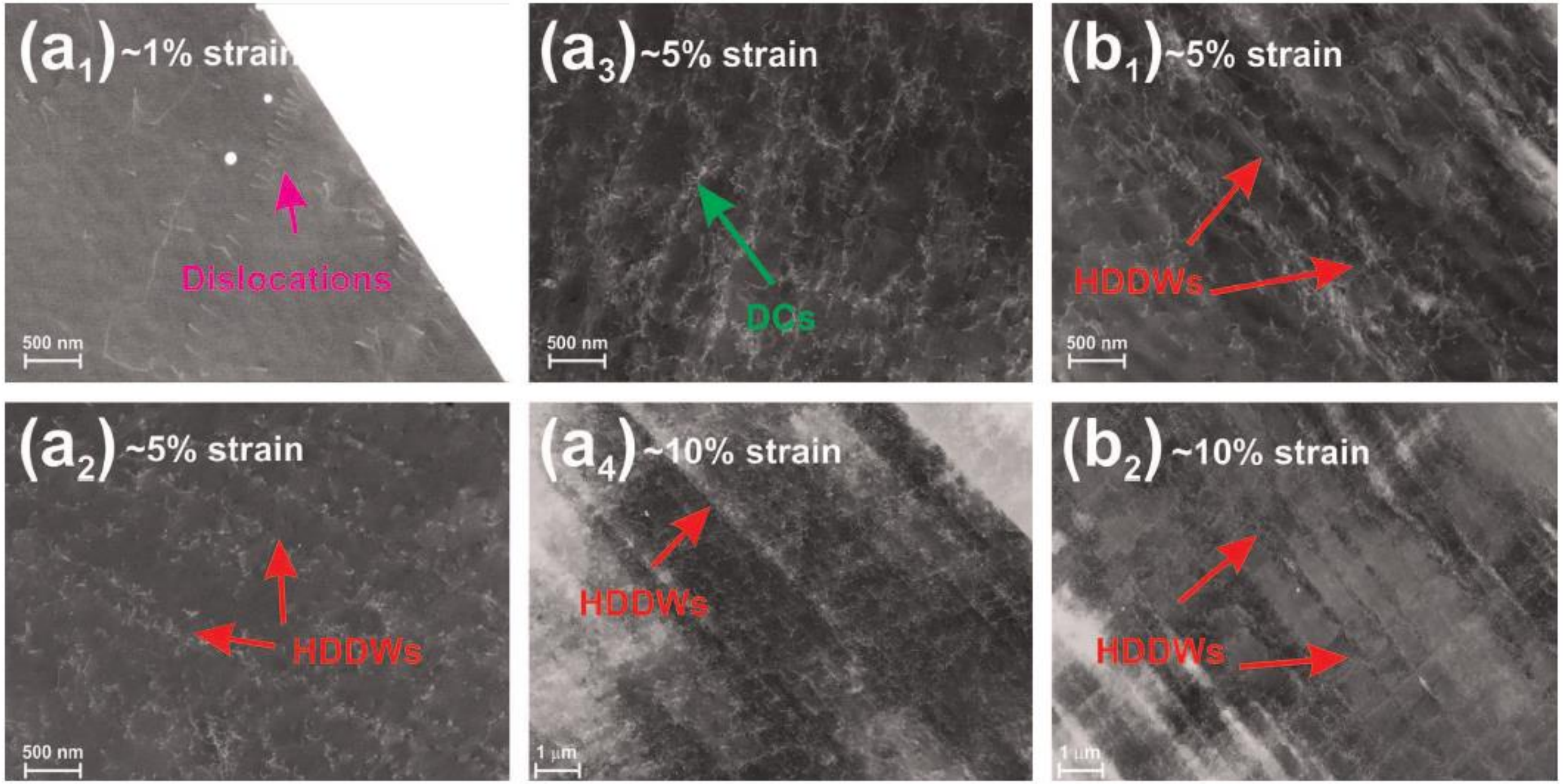

Fig. 8. Deformation substructures revealed by electron scanning contrast imaging for the representative (a) 21Mn and (b) 38Mn at different strain levels of 1%, 5% and 10%.

Planar slip in a CoCrFeMnNi alloy

Materials Science & Engineering A 648 (2015) 183–192

Contents lists available at ScienceDirect

Materials Science & Engineering A

journal homepage: www.elsevier.com/locate/msea

Non-equiatomic high entropy alloys: Approach towards rapid alloy screening and property-oriented design

K.G. Pradeep [a,b], C.C. Tasan [a,*], M.J. Yao [a], Y. Deng [a,c], H. Springer [a], D. Raabe [a,*]

[a] Max-Planck-Institut für Eisenforschung GmbH, Max-Planck-str.1, 40237 Düsseldorf, Germany
[b] Materials Chemistry, RWTH Aachen University, Kopernikusstr.10, 52074 Aachen, Germany
[c] Department of Engineering Design and Materials, Norwegian University of Science and Technology, No-7491 Trondheim, Norway

Dislocations progress to dislocation cells (DC) and high density dislocation walls (HDDW)

Summary

Defect imaging via SEM – highly accessible via electron channeling

- FEG SEM + BSE Detector
- Must consider crystallography → **g** vector and defect geometry

Opportunities for progress

- Improved BSE detector sensitivity
- Coordination with *in situ* methods inside the SEM
- Coordination with SPM and other SEM modes → defect-property correlations
- Automated high-speed imaging and mapping of millimeter areas
- Reliable defect identification → accurate simulations
- Reliable **g** vector control → informed by EBSD and/or SACP

I recommend this review article:

Theory and application of electron channelling contrast imaging under controlled diffraction conditions

Acta Materialia 75 (2014) 20–50

Stefan Zaefferer*, Nahid-Nora Elhami

Max-Planck-Institute for Iron Research, Dusseldorf, Germany

Become a ECAMT-FIG Member

Join us at our next
ECAMT-FIG Business Meeting
Tuesday, July 26
12:15-1:15 pm
Room C223

Organizers:
Jorg Wiezorek, University of Pittsburgh
Yoosuf Picard, Carnegie Mellon University
Robert Stroud, NanoMegas
Sergei Roviumov, University of Notre Dame

A Pre-Meeting Congress
hosted by the MSA Electron Crystallography and
Automated Mapping Techniques -- Focused Interest Group

Exploiting the Diffractive Properties of Electrons for Solving Materials Problems

FEI
HITACHI Inspire the Next
NANOMEGAS USA
ZEISS
GATAN
FISCHIONE INSTRUMENTS
JEOL
EDAX Smart Insight
TESCAN PERFORMANCE IN NANOSPACE
OXFORD INSTRUMENTS

M&M 2016
MICROSCOPY & MICROANALYSIS
July 24-28, 2016 • Columbus, Ohio

MSA Microscopy Society of America

Become a ECAMT-FIG Member

Join us at our next
ECAMT-FIG Business Meeting
Tuesday, July 26
12:15-1:15 pm
Room C223

Today's slides will be posted for ECAMT-FIG members
[FUTURE ACTIVITIES / NEW RESOURCES]

http://www.microscopy.org/communities/ecamt_fig.cfm

The **Electron Crystallography & Automated Mapping Techniques Focused Interest Group (ECAMT-FIG)** is a community of MSA members with a common interest in crystallography and advanced electron methods for materials characterization. Our goal is to provide a platform for the distribution and discussion of ECAMT-relevant information chosen by the membership. Our activities include the hosting of pre-meeting congresses and symposia during the annual M&M meeting. We also host a luncheon and business meeting during the annual M&M meeting.

ypicard@cmu.edu
ECAMT-FIG Leader-Elect

Microscopy Society of America